Optics of Marine Particles

Dariusz Stramski

Scripps Institution of Oceanography
University of California San Diego
Email: dstramski@ucsd.edu

IOCCG Summer Lecture Series

18 July - 29 July 2020, Villefranche-sur-Mer, France

Seawater is a complex optical medium with a great variety of particle types and soluble species

- Molecular water
- Inorganic salts
- Dissolved organic matter

Suspended Particulate Matter

- Plankton microorganisms
- Organic detrital particles
- Mineral particles
- Colloidal particles
- Air bubbles

A great variety of biological and mineral particle types which absorb and scatter light differently

Mineral particles

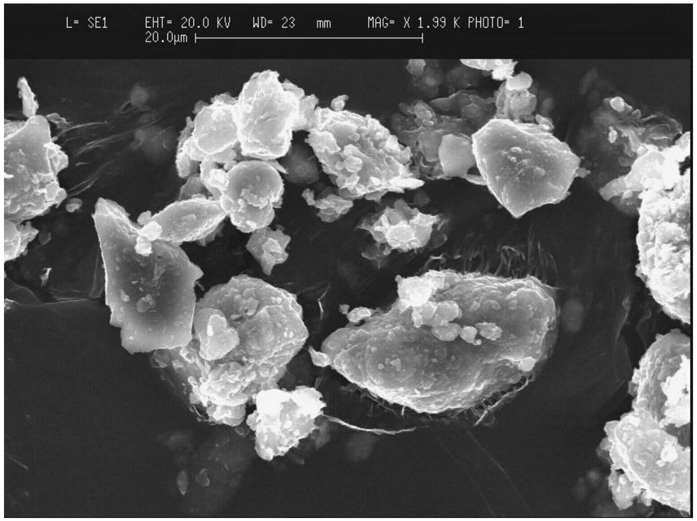

Colloids / nanoparticles

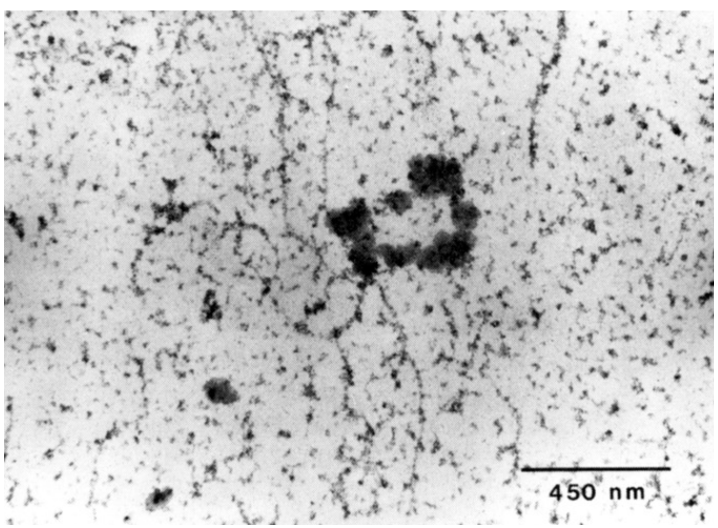

Plankton microorganisms

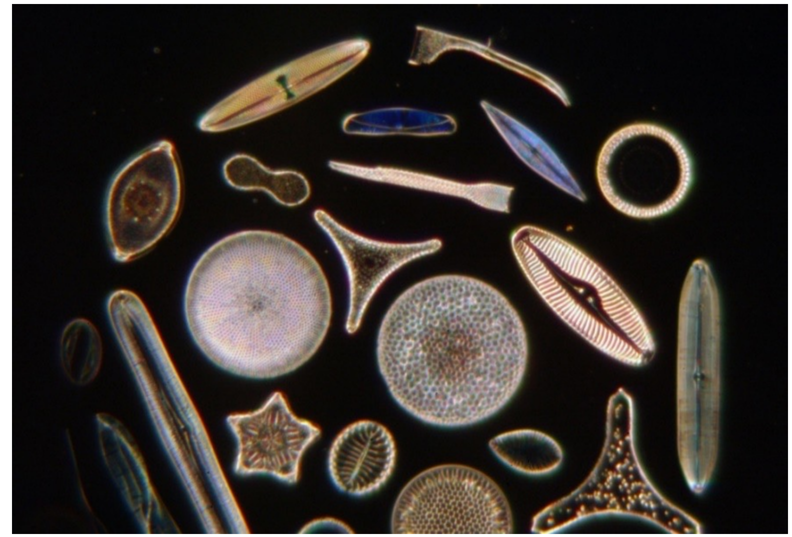

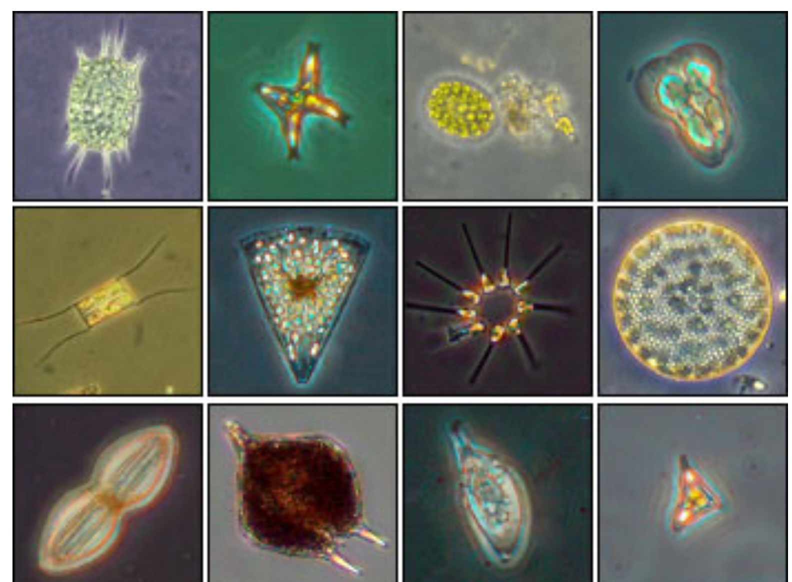

Fundamentals of single-particle optics and the linkage between the single-particle and bulk optical properties of particle suspension

Defining the bulk inherent optical properties (IOPs)

A small water volume ΔV contains an assemblage of many particles (and molecules)

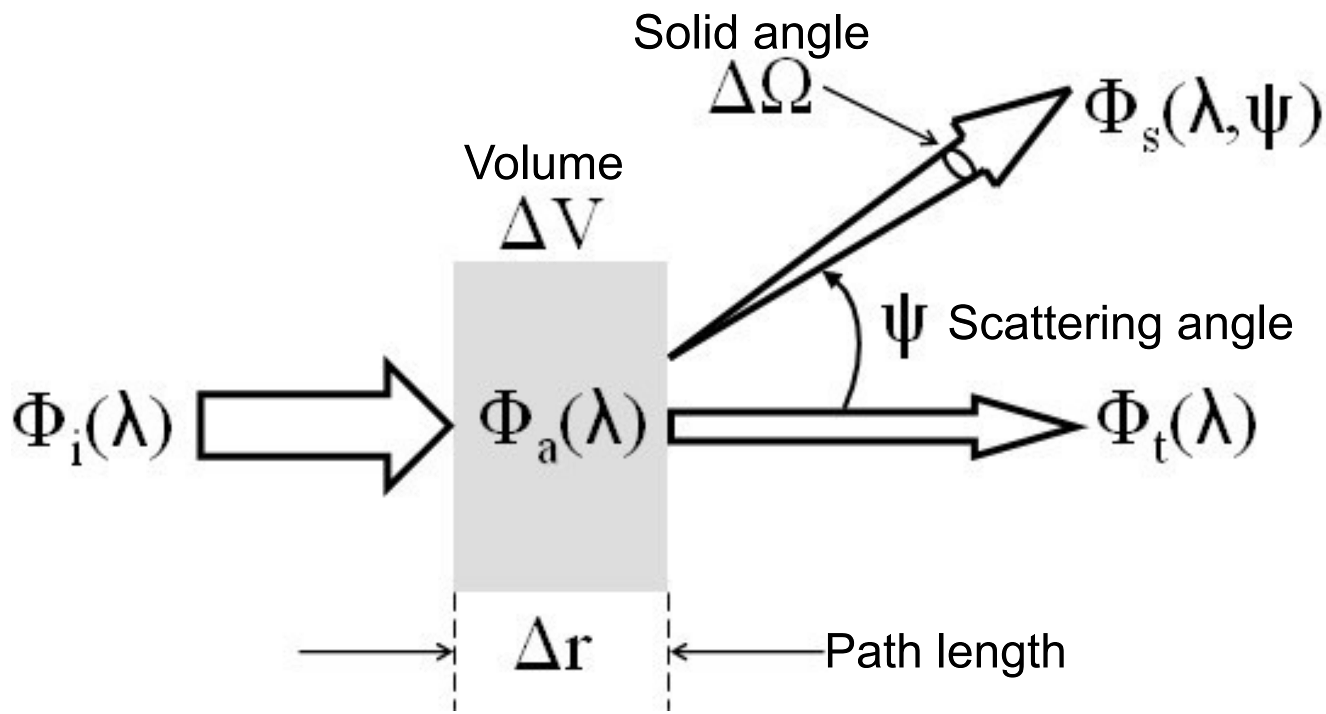

$\Phi_i(\lambda)$ Incident spectral power (flux); alternative symbols $F_i(\lambda)$ or $F_o(\lambda)$

$\Phi_t(\lambda)$ Directly transmitted spectral power; alternative symbol $F_t(\lambda)$

$\Phi_a(\lambda)$ Absorbed spectral power; alternative symbol $F_a(\lambda)$

$\Phi_s(\lambda)$ Total spectral power scattered out of the beam; alternative symbols $F_s(\lambda)$ or $F_b(\lambda)$

$$\Phi_i(\lambda) = \Phi_a(\lambda) + \Phi_s(\lambda) + \Phi_t(\lambda)$$

(Mobley,1994)

Operational definitions of basic IOP coefficients

Bouger – Lambert exponential law for absorption

Absorption coefficient $a = -\frac{1}{R} \ln\left(\frac{\Phi_t + \Phi_s}{\Phi_i}\right)$ (in units of m^{-1} if pathlength *R* is in units of m)

$$\boxed{\Phi_t + \Phi_s = \Phi = \Phi_i\, e^{-a R}}$$

Exponential law for beam attenuation

Beam attenuation coefficient $c = -\frac{1}{R} \ln\left(\frac{\Phi_t}{\Phi_i}\right)$ (in units of m^{-1})

$$\boxed{\Phi_t = \Phi = \Phi_i\, e^{-c R}}$$

Scattering coefficient: $b = c - a$

Note: The inherent angular scattering property is the volume scattering function (here omitted for brevity but presented in detail in other lectures)

Imperfect geometry for measuring the absorption coefficient $a(\lambda)$

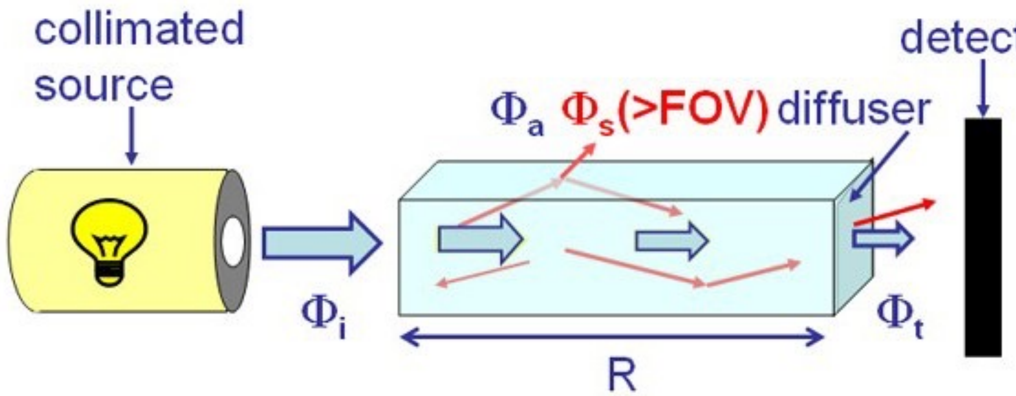

This detector collects only forward scattered light within the detector's FOV (field of view). This results in overestimation of measured absorption coefficient.

$$a = -\frac{1}{R} \ln\left(\frac{\Phi_t + \Phi_s(\mathrm{FOV})}{\Phi_i}\right)$$

Φ_s(>FOV) contributes to scattering error of absorption measurement.
As a result, the absorption coefficient is overestimated.

Perfect absorption measurement if FOV allows detection of all scattered power Φ_s

Geometry for measuring the beam attenuation coefficient $c(\lambda)$

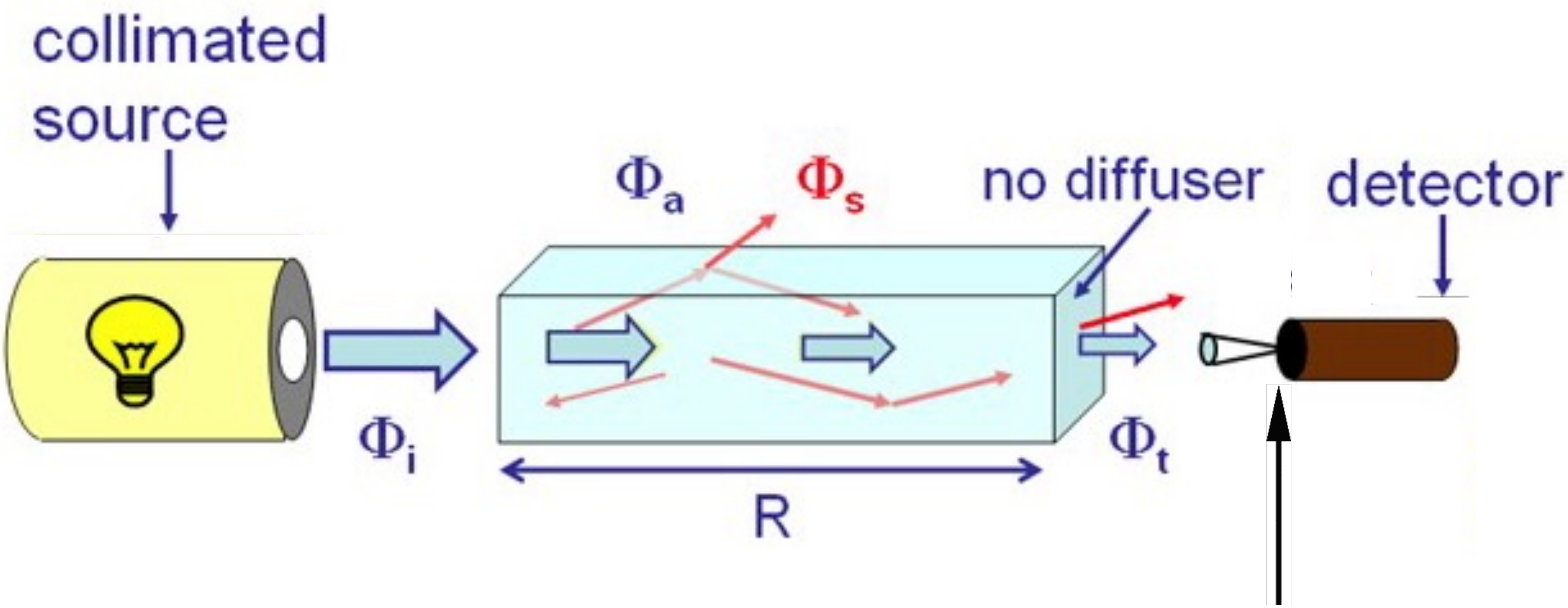

This detector has a narrow field of view (FOV < 1°). Ideally, it should measure only directly transmitted light, Φ_t, and omit scattered light.

In reality, small but finite field of view results in underestimation of the beam attenuation coefficient

Linkage between the single-particle optical properties and bulk optical properties of particle suspension

This is an example relationship for light absorption properties assuming that the bulk absorption coefficient represents a collection of identical particles (similar relationships can be written for light scattering and attenuation properties)

$$a = (N/V)\, Q_a\, G = (N/V)\, \sigma_a \qquad\qquad \sigma_a = a\,/\,(N/V)$$

Bulk properties:

a is the bulk absorption coefficient of a collection of identical particles in aqueous suspension (units of m^{-1})

N/V is the number of particles per unit volume of water (units of m^{-3})

Single-particle properties:

Q_a is the absorption efficiency factor (dimensionless) – defined on the next slide

σ_a (= $Q_a\, G$) is the absorption cross-section (units of m^2)

G is the area of geometric cross-section of particle (units of m^2)
For spherical particle $G = (\pi/4)D^2$ where D is a diameter

Note: a, Q_a, and σ_a are the spectral quantities (i.e., they are functions of light wavelength λ)

Absorption efficiency factor for a single particle

$$Q_a(\lambda) = F_a(\lambda) \,/\, F_o(\lambda)$$

$F_o(\lambda)$ - spectral radiant power intercepted by geometrical cross-section of particle

$F_a(\lambda)$ - spectral radiant power absorbed by particle

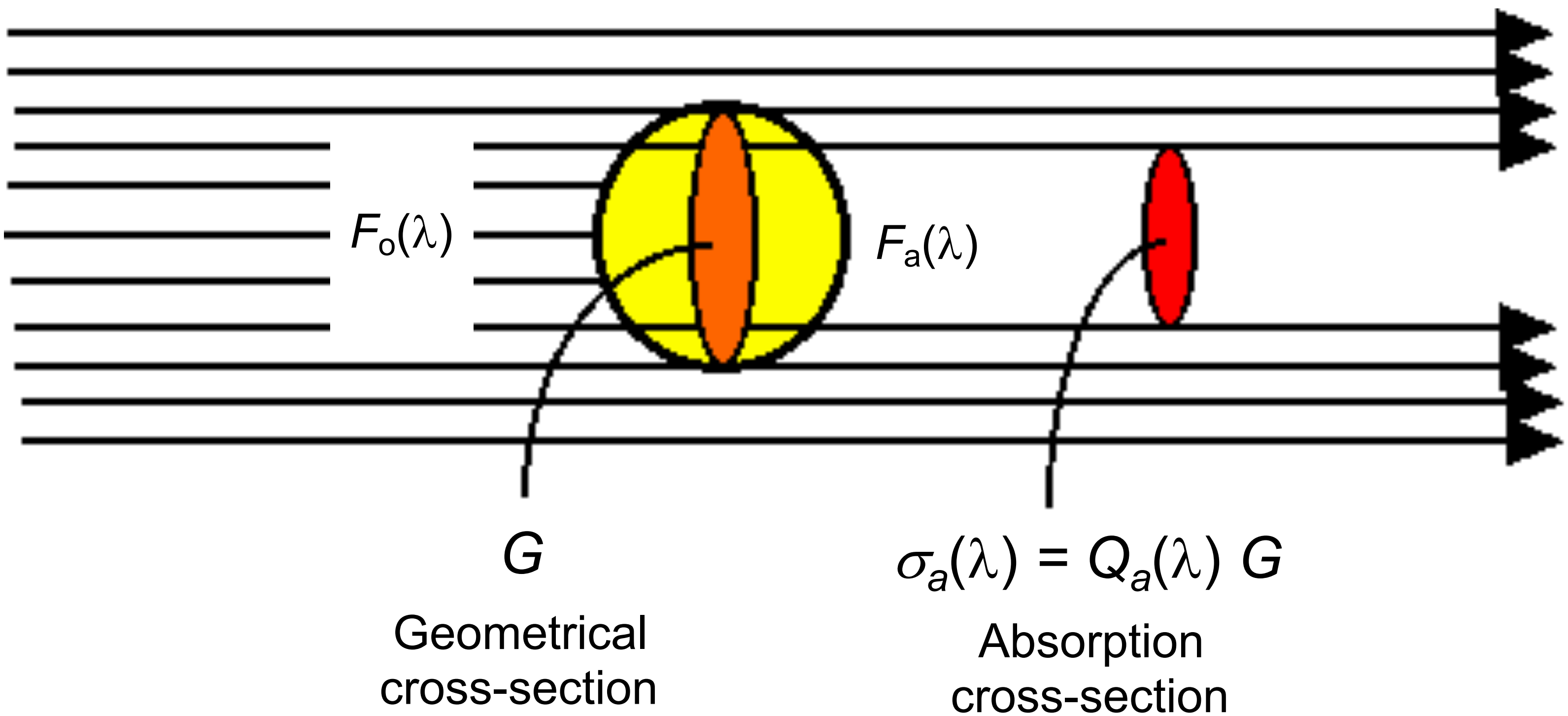

Theoretical dependence of absorption efficiency on particle properties parameterized in terms of "absorption thickness" ρ'

For a particle suspended in water

$$\rho' = 4\,\alpha\, n' = a_s\, D$$

where the particle size parameter α is

$$\alpha = (\pi\, D\, n_w) / \lambda$$

and the imaginary index of refraction of particle is

$$n' = (a_s\, \lambda) / (4\,\pi\, n_w)$$

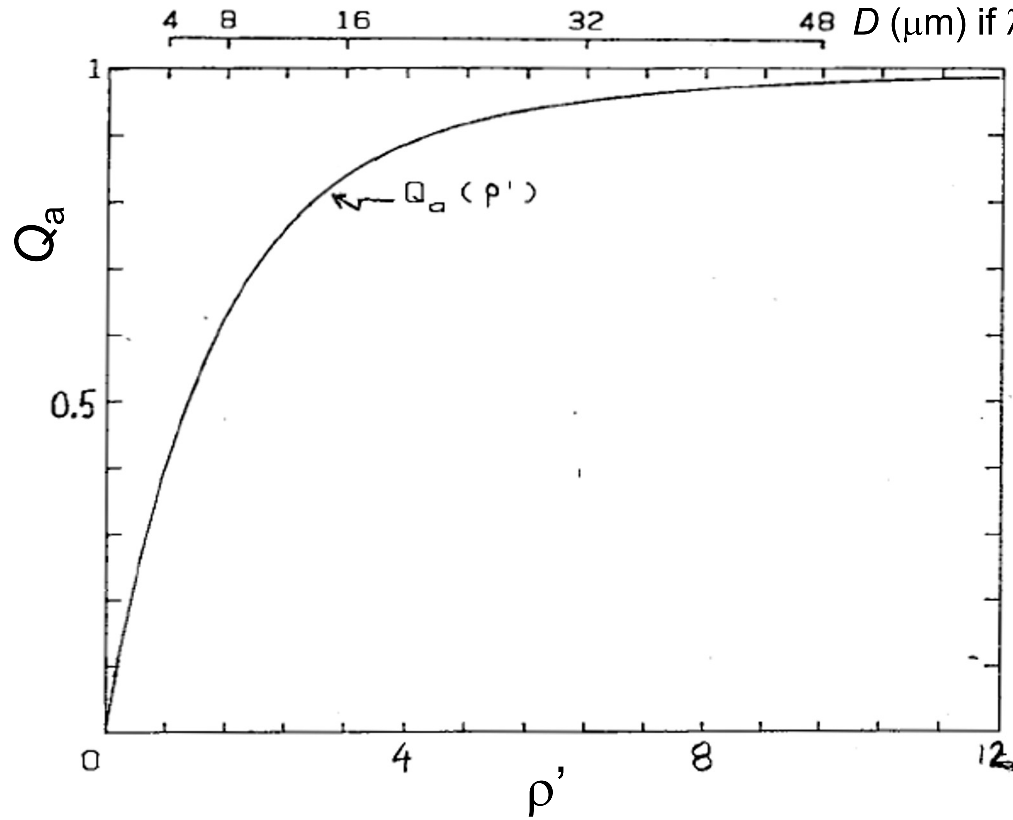

$a_s(430)=$ 2×10^5 m^{-1} for typical phytoplankton cell

a_s (m^{-1}) is the absorption coefficient of substance forming the particle; D (m) is the particle diameter; and n_w is the refractive index of water

Note: ρ', α and n' are dimensionless; symbol x is often used in literature instead of α
Q_a, a_s, and n' are all functions of λ

(Morel and Bricaud 1981)

Example spectra of absorption efficiency factor for two phytoplankton species derived from laboratory measurements of $a(\lambda)$ and cell size distribution made on cultures

The *mean* efficiency factor, $\overline{Q_a}$, represents an "*average"* phytoplankton cell derived from the actual population of cells that exhibit a certain size distribution. Because the size distribution is narrow the mean is meaningful in a sense that it represents an "*average*" cell within a population of similar cells.

Mean absorption efficiency factor $\overline{Q_a}$

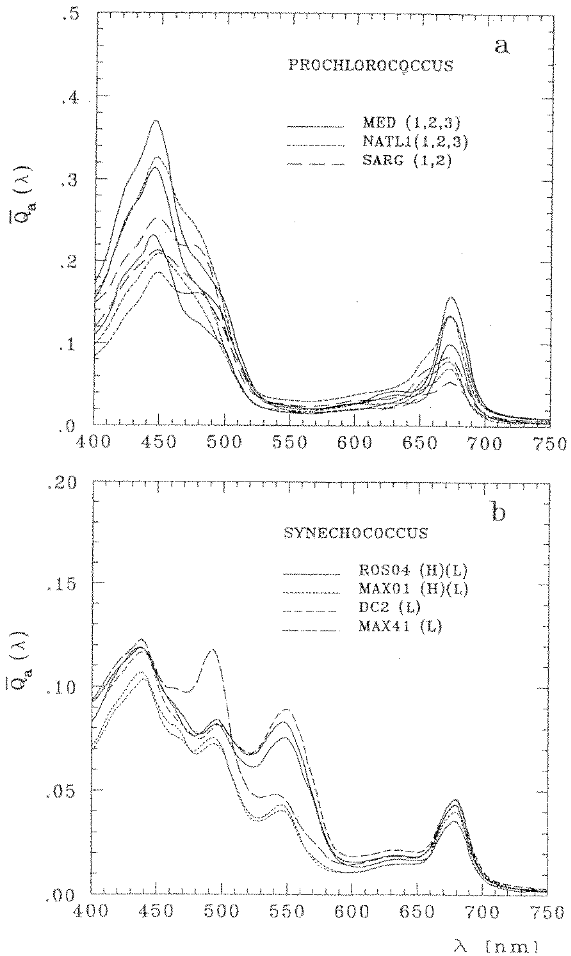

Size distribution $N(D)/V$

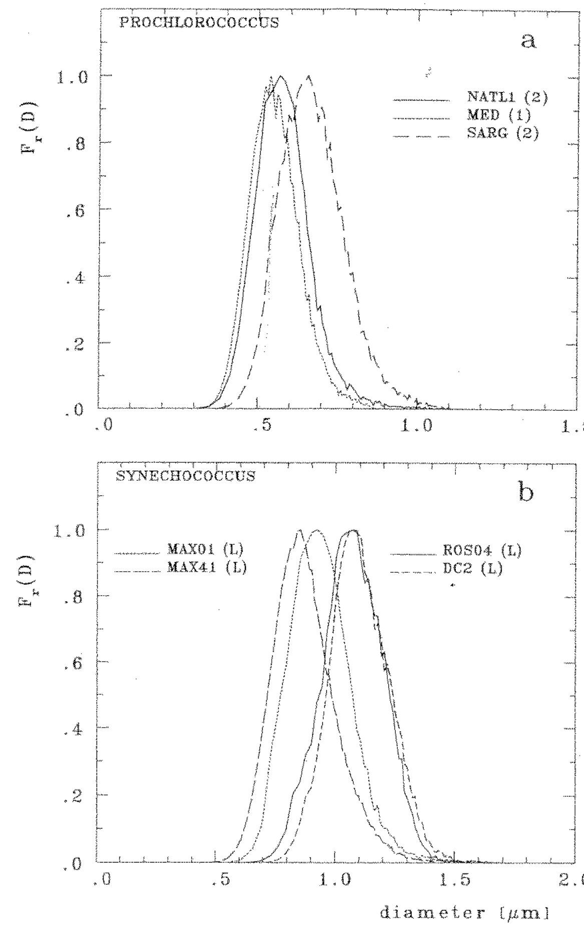

(Morel et al. 1993)

Comparison of experimental data of absorption efficiency for various phytoplankton and heterotrophic microorganisms with theoretical curve

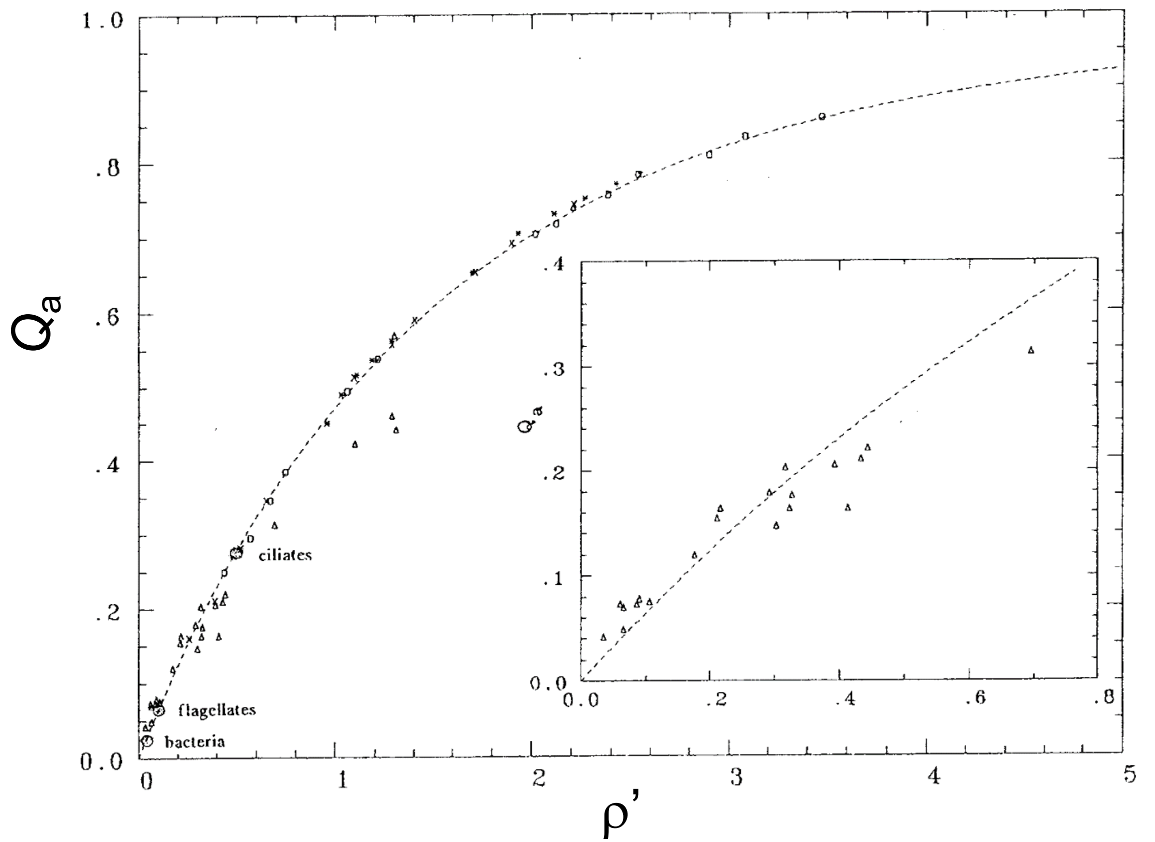

Figure 1. The theoretical variations of Q_a, the efficiency factor for absorption (dashed curves), as a function of the dimensionless parameter ρ',. The triangles are experimental determinations of Q_a (at 675 nm) for various algae (Morel and Bricaud, 1986; Ahn, 1990); other symbols are for determinations of 3 algal species studied by Sosik (1988). The values for heterotrophic organisms, as indicated, come from Morel and Ahn (1990, 1991). The inset is an enlargment of the initial part of the curve.

(Morel 1991)

Scattering efficiency factor for a single particle

$$Q_b(\lambda) = F_b(\lambda) / F_o(\lambda)$$

$F_o(\lambda)$ - spectral radiant power intercepted by geometrical cross-section of particle

$F_b(\lambda)$ - spectral radiant power scattered by particle in all directions

differential contribution from one example scattering angle ψ, $\Delta F_b(\lambda,\psi)$

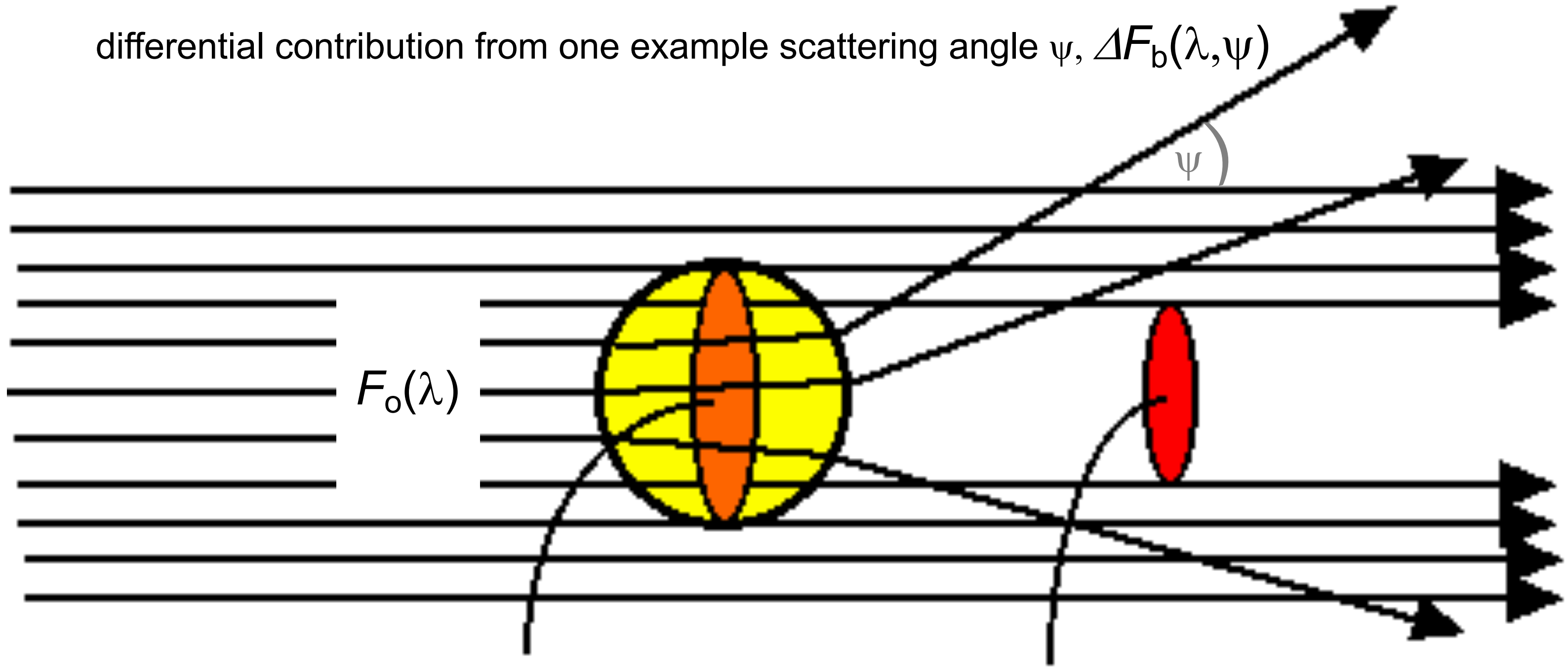

G

Geometrical cross-section

$\sigma_b(\lambda) = Q_b(\lambda)\ G$

Scattering cross-section

Note: ψ-dependent differential scattering efficiency and cross-section can also be defined

Theoretical dependence of optical efficiency factors on particle properties parameterized in terms of phase shift parameter ρ

$\rho = 2\,\alpha\,(n - 1)$ where *n* is the refractive index of particle relative to water

Absorption efficiency $Q_a = F_a/F_o$

Scattering efficiency $Q_b = F_b/F_o$

Attenuation efficiency $Q_c = F_c/F_o$

$F_c = F_a + F_b$

$Q_c = Q_a + Q_b$

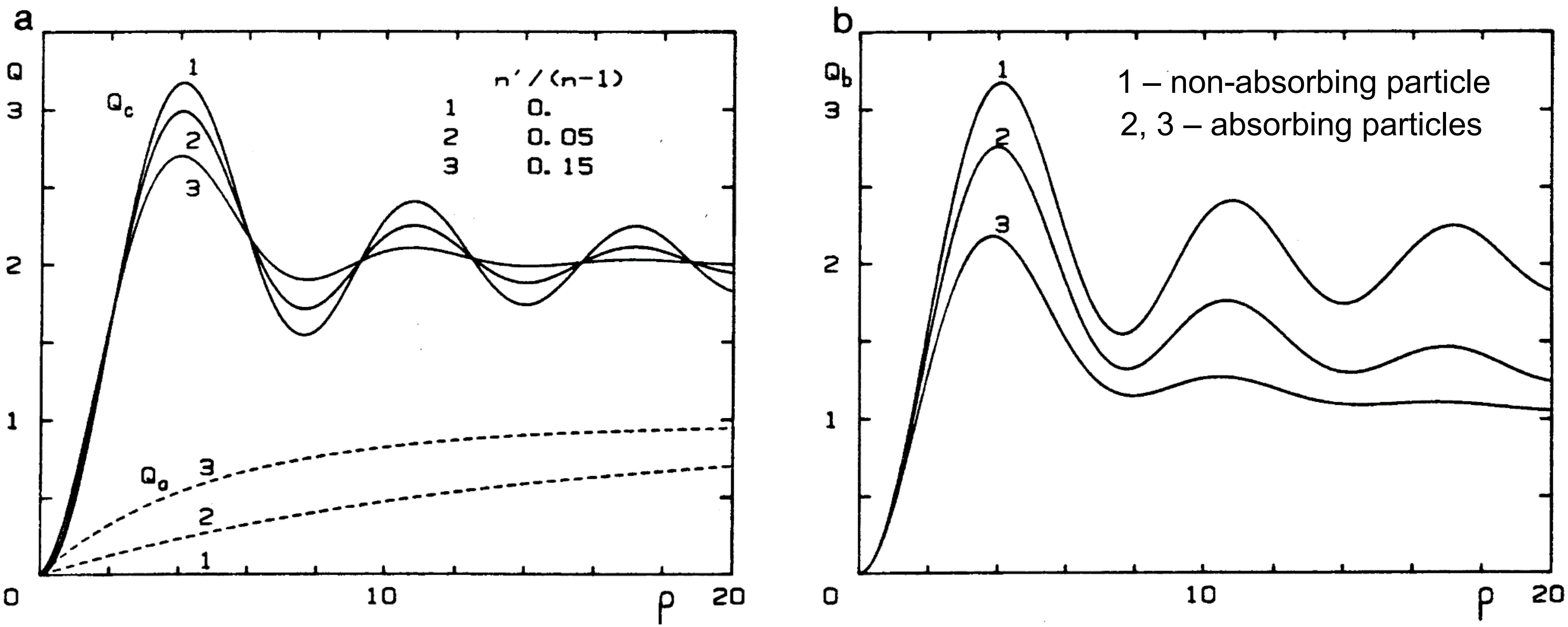

FIG. 3. Variations of the efficiency factors for attenuation, Q_c, *for absorption*, Q_a (a), and for scattering, Q_b (b) vs. the parameter $\varrho = 2\,\alpha(n-1)$, for increasing values of the ratio $n'/(n-1)$ where *n* and *n'* are the real and imaginary parts of the relative refractive index of the particles.

(Morel and Bricaud 1986)

Scattering by a single particle: Phase shift parameter

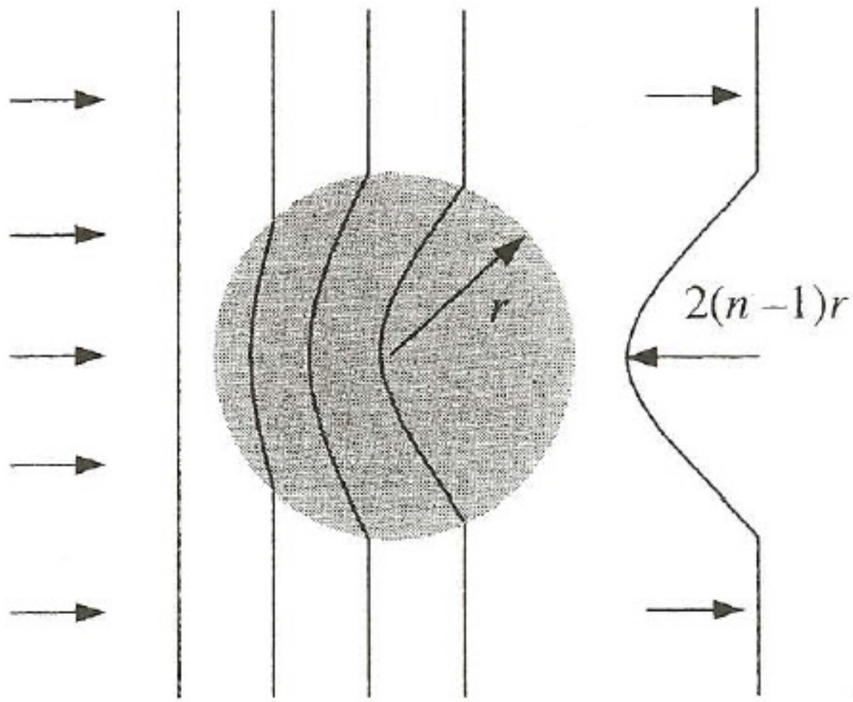

Figure 3.5. Phase fronts of a light wave traveling through a sphere of radius r. The wave slows down while traveling through the particle. The accumulated phase difference is proportional to the total distance traveled through the particle and is a function of the point of entry. The phase difference between the light passing through the center of the sphere and the light passing outside the sphere is $2(n-1)r$.

(Jonasz and Fournier 2007)

The effect of polydispersion on attenuation efficiency

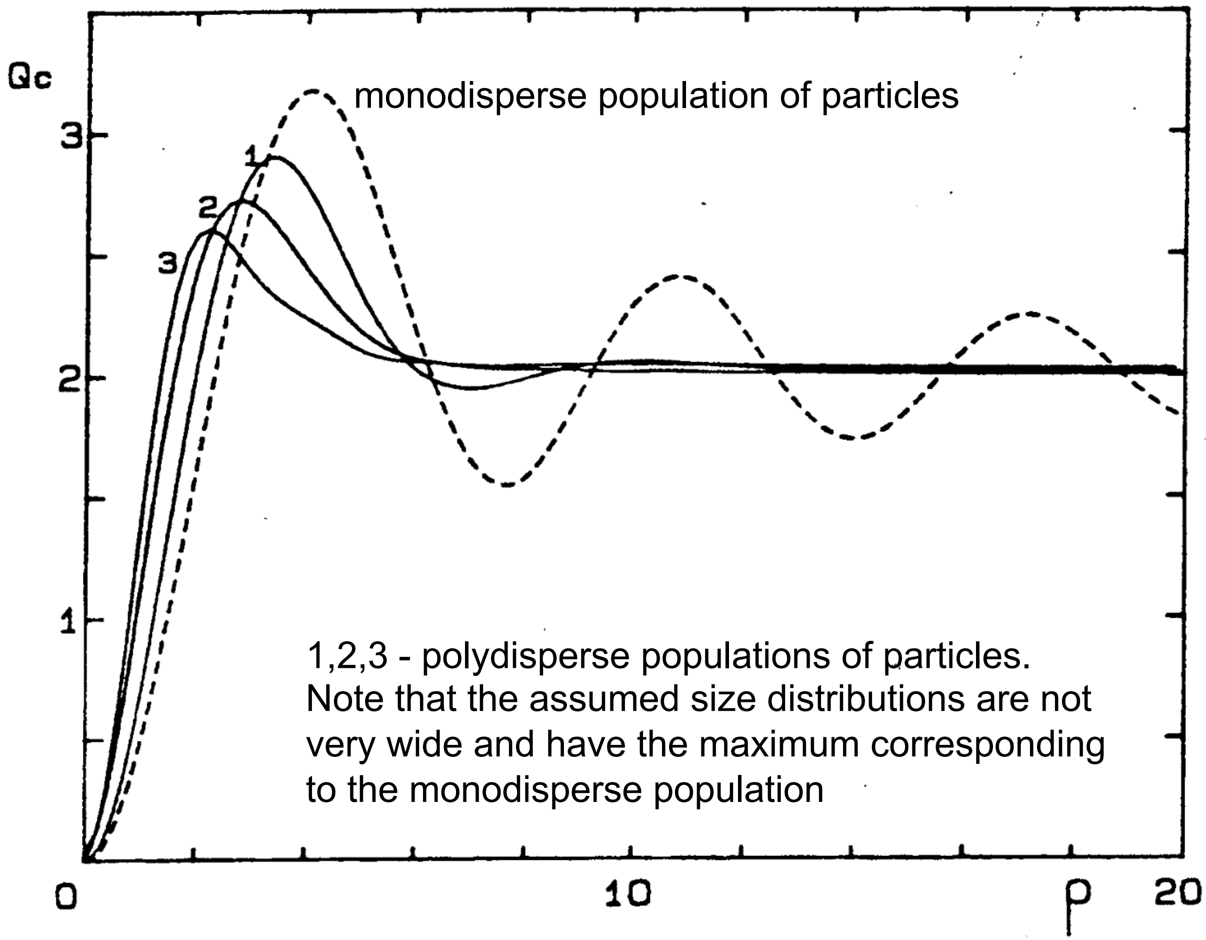

FIG. 4. Mean efficiency factor for attenuation Q_c of a "mean" particle representative of a polydispersed population, plotted as a function of ϱ_m, *the* ϱ value which corresponds to the maximum of the size distribution function $F(\varrho)$ (see Equation 17). The index of refraction is real (no absorption) and the curves 1 and 3 correspond to log-normal distributions such as $F(\varrho_M/2) = F(2\varrho_M)$ = respectively 0.01, 0.1, 0.3 $F(\varrho_M)$. The dashed curve, redrawn from Fig. 3 for $n' = 0$, represents the limiting case of a population of monosized particles.

(Morel and Bricaud 1986)

Scattering and backscattering efficiencies versus particle size

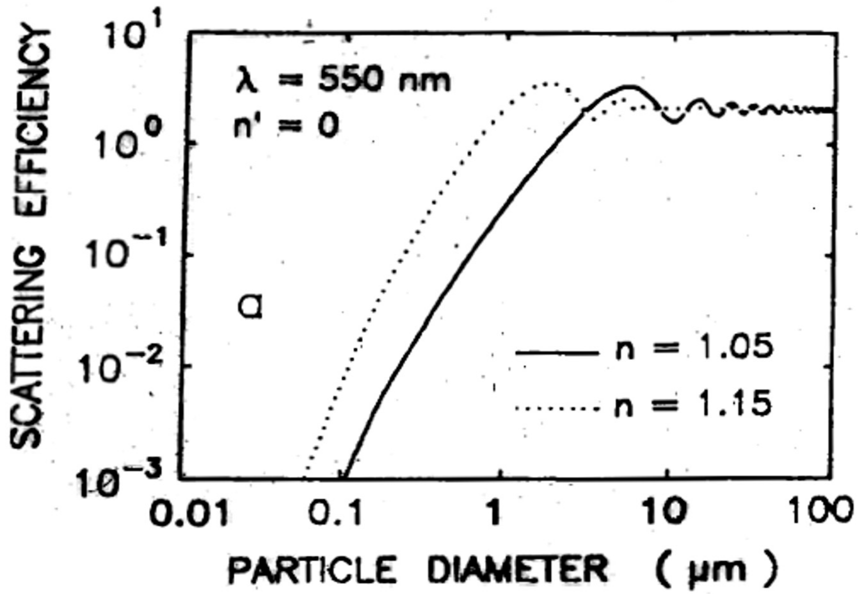

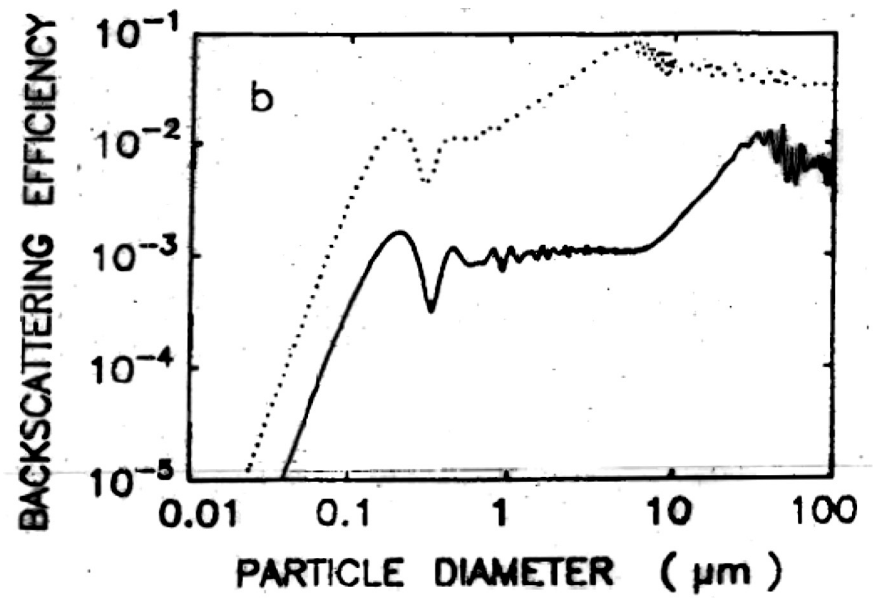

Note: For the purpose of this illustration, the light wavelength (λ) and the particle refractive index (*n*, *n*’) are fixed at selected values as indicated. Backscattering efficiency represents the entire range of backscattering angles from 90^o to 180^o.

(Stramski and Kiefer 1991)

Comparison of experimental data of scattering efficiency for various phytoplankton and heterotrophic microorganisms with theoretical curves

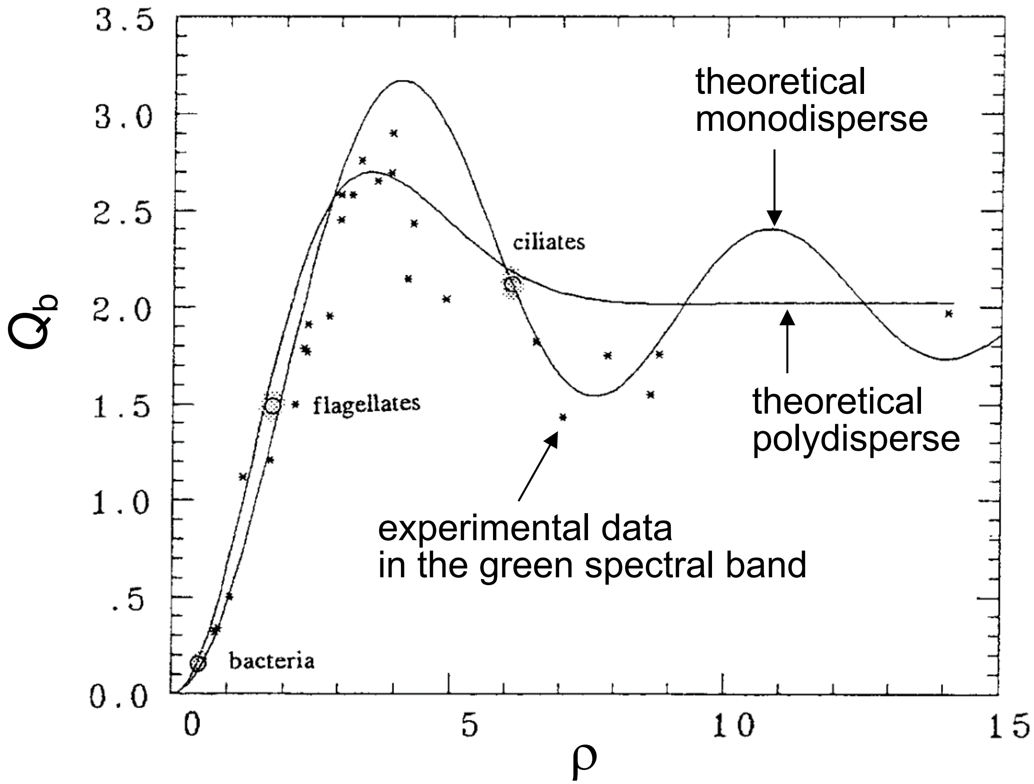

Figure 2. The theoretical variations of Q_b, the efficiency factor for scattering by non absorbing spheres (solid curve with marked oscillations) as a function of the dimensionless parameter ρ. The smoothed curve is for an averaged $\bar{Q}_b$ to be applied for population with a log - normal size distribution. The crosses are the $\bar{Q}_b$ values (at $\lambda \sim 580$ nm) determined for various phytoplankters grown in culture (see Table 1 in Morel and Bricaud, 1986); additional data for algal cells come from Ahn (1990). The circles indicate the $\bar{Q}_b$ values (at $\lambda \sim 550$ nm) determined for free living marine bacteria, heterotrophic flagellates, and naked ciliates, (Morel and Ahn, 1990; 1991).

(Morel 1991)

Spectra of scattering efficiency for various phototrophic and heterotrophic microorganisms derived from measurements

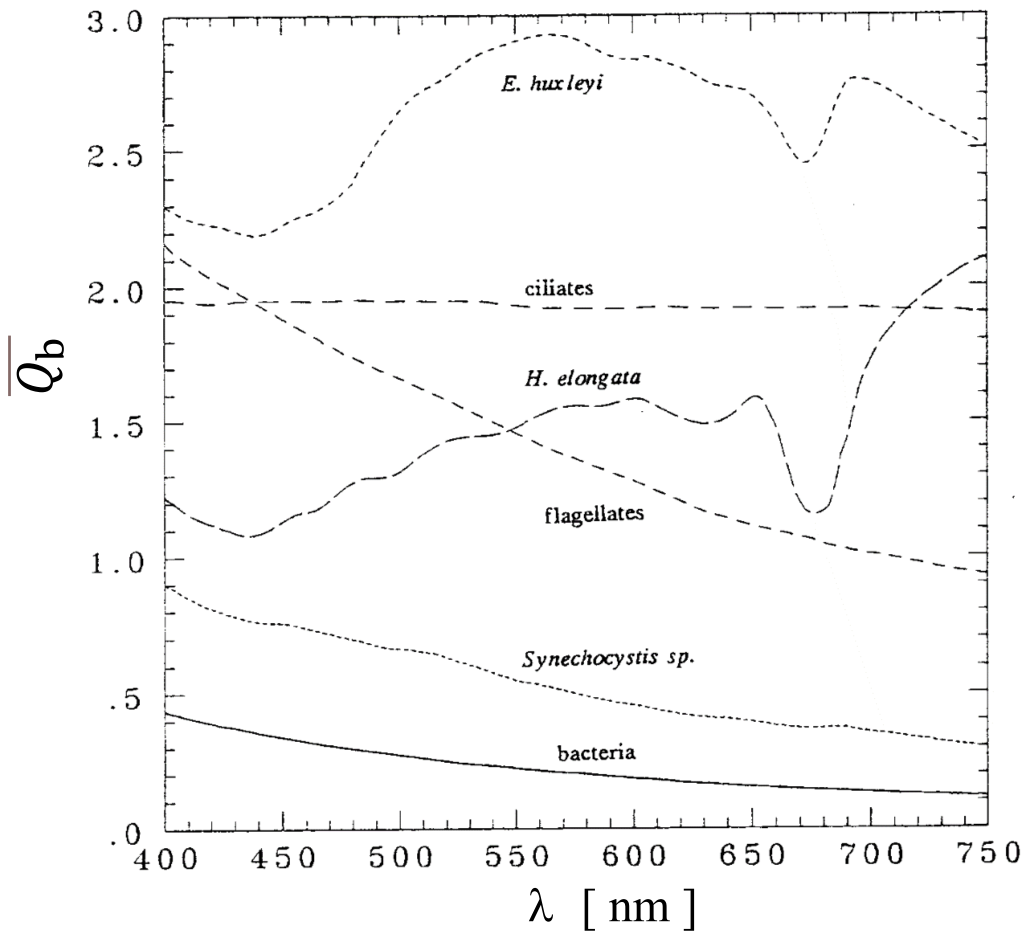

Note: Ciliates are the largest particles (~30 μm) in this comparison

Note: Bacteria are the smallest particles (~0.5 μm)

Figure 3. Spectral variations of Q_b within the 400-750 nm range of various phototrophic and heterotrophic organisms as experimentally determined (Morel and Ahn, 1990, 1991).

(Morel 1991)

D = 3.4 μm
n = 1.07

for visible light:

α = 20 – 35

ρ = 3 – 5

Optical efficiency factors Q_c, Q_b, and Q_a :

Examples for monospecific cultures of phytoplankton cells

(derived from laboratory measurements of absorption and attenuation coefficients, and size distribution made on cultures)

D = 1.2 μm
n = 1.0325

for visible light:

α = 7 – 13

ρ = 0.5 – 1.5

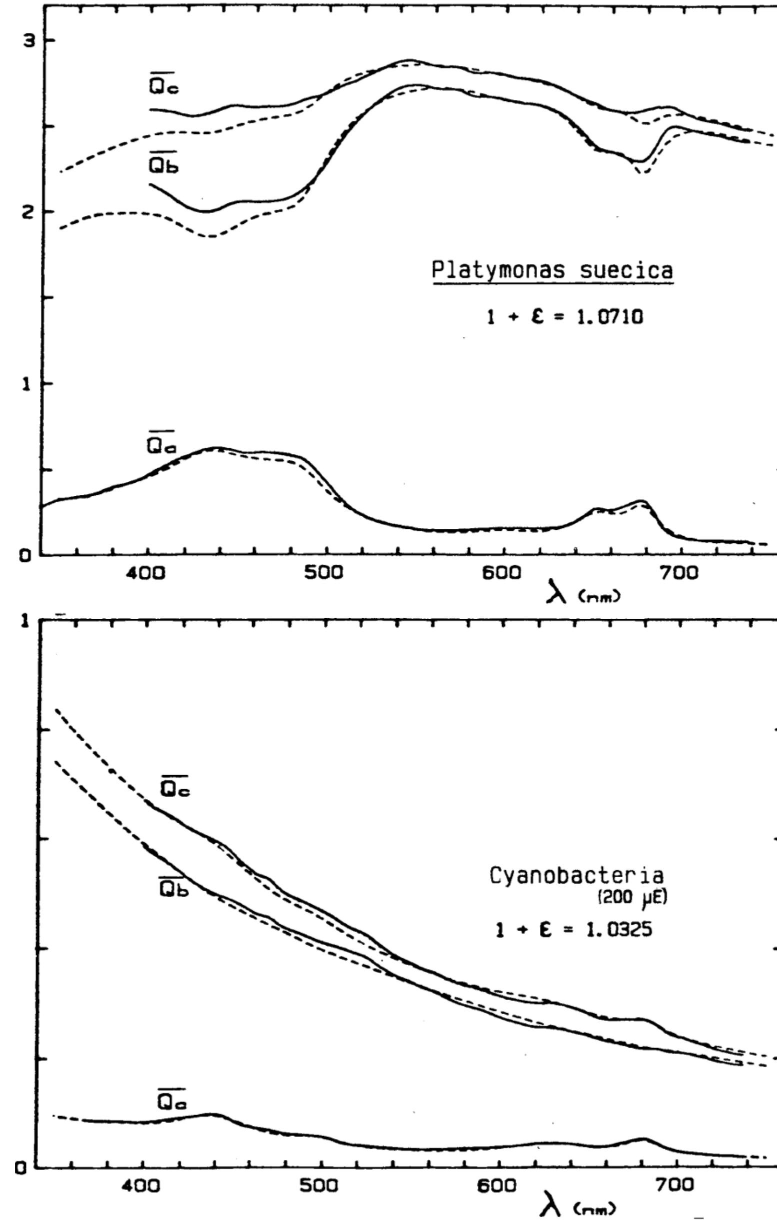

FIG. 14. Spectral variations of the mean efficiency factors for attenuation ($\overline{Q_c}$), scattering ($\overline{Q_b}$) and absorption ($\overline{Q_a}$), deduced from the attenuation and absorption coefficients experimentally determined (continuous lines), for two phytoplanktonic species. The variations of $\overline{Q_c}$, $\overline{Q_b}$ and $\overline{Q_a}$ obtained from a theoretical model (see text) are shown as dashed lines. The central value of the real part of the refractive index, $1 + \epsilon$, leading to the best theory/experiment agreement is indicated on the Figures.

(Morel and Bricaud 1986)

The spectral behavior of scattering efficiency is affected by anomalous dispersion of the particle refractive index (*n*) within the absorption band (*n*')

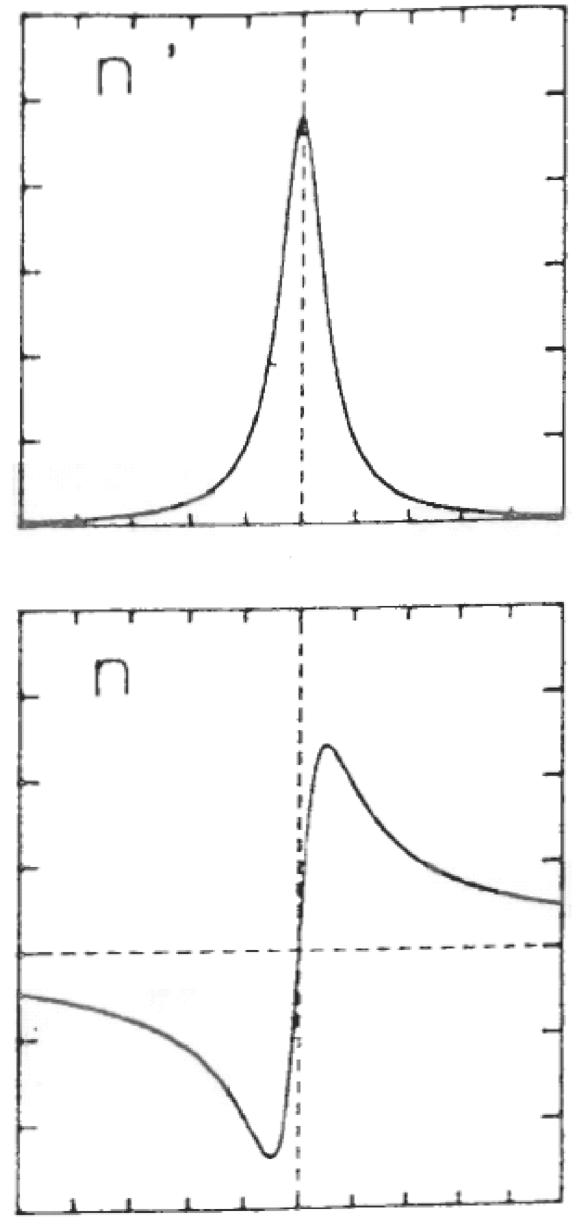

Light wavelength

(Morel and Bricaud 1986)

Measuring the volume scattering function $\beta(\psi,\lambda)$

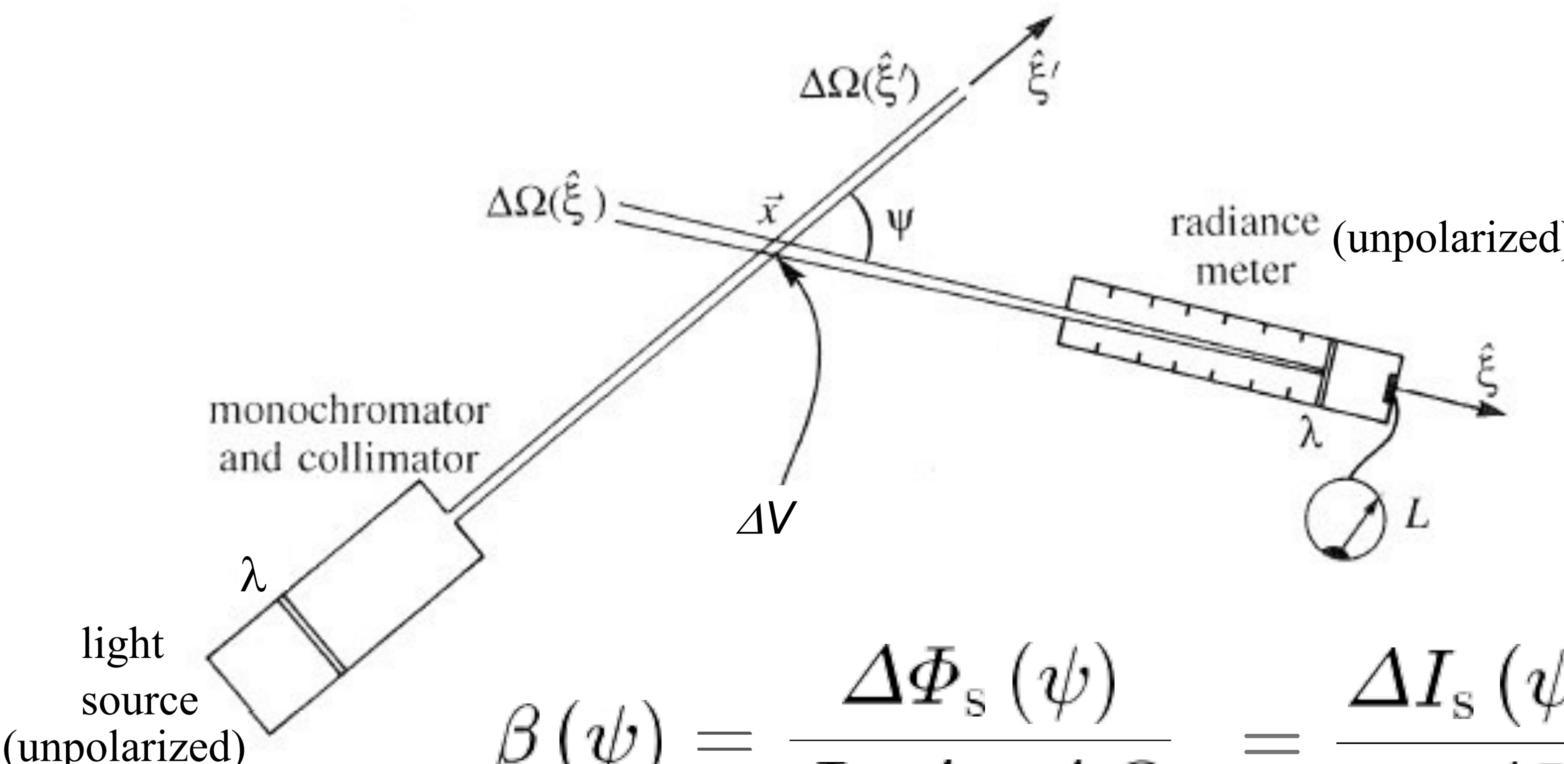

$$\beta(\psi) = \frac{\Delta\Phi_{\mathrm{s}}(\psi)}{\Phi_{\mathrm{i}}\ \Delta r\ \Delta\Omega} = \frac{\Delta I_{\mathrm{s}}(\psi)}{E_{\mathrm{i}}\ \Delta V}$$

λ light wavelength

ψ scattering angle

ΔV scattering volume

Δr path length within scattering volume

Φ_{i} incident power

E_{i} incident irradiance

$\Delta\Phi_{\mathrm{s}}(\psi)$ scattered power

$\Delta I_{\mathrm{s}}(\psi)$ scattered intensity

$\Delta\Omega$ solid angle of scattering detector

Scattering phase function: Effect of polydispersion

$\bar{\beta} = \beta / b$

ψ and λ arguments omitted for brevity

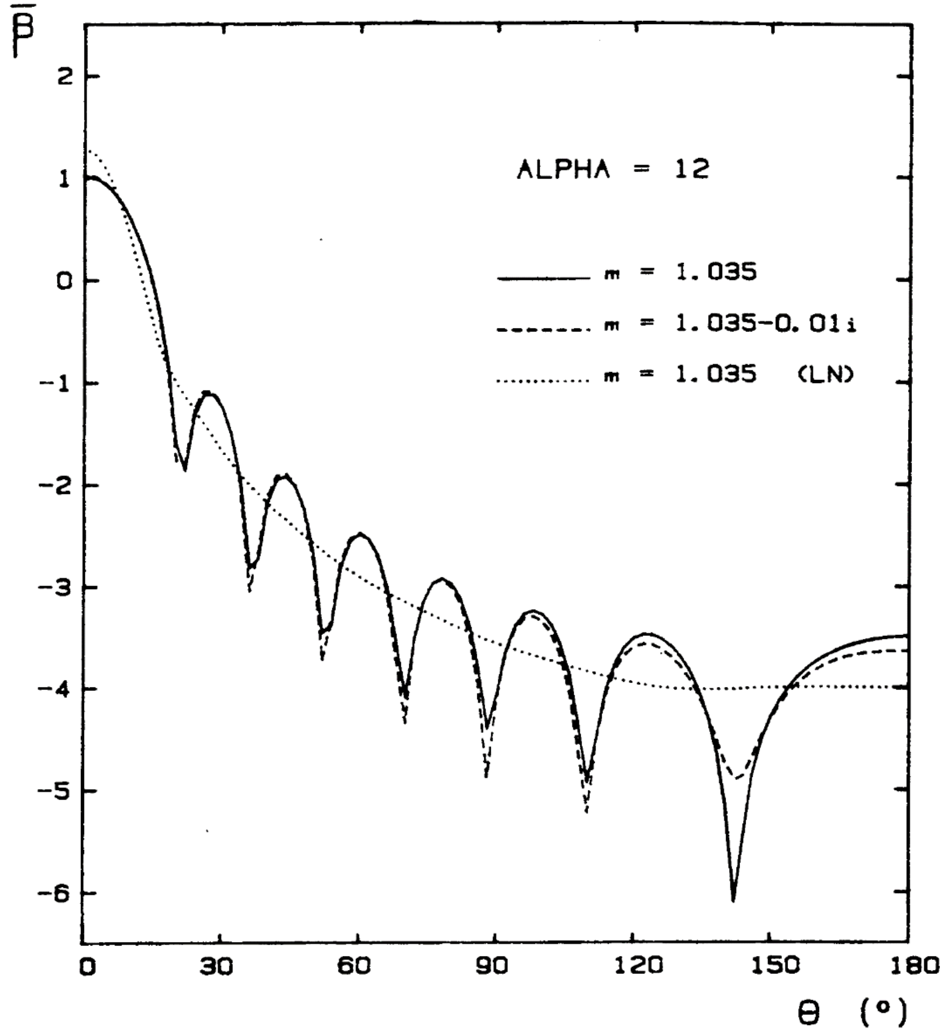

FIG. 5. Normalized volume scattering functions, $\bar{\beta}(\theta)$ (Equations 5′ and 18), for a particle of relative size $\alpha = 12$, when the refractive index is 1.035 and 1.035–0.01 *i*. The dotted curve represents the same $\bar{\beta}(\theta)$ function for a polydispersed population of particles with $n = 1.035$, computed according to Equation 20. The size distribution function $F(\alpha)$ is a log-normal law such that the modal relative size $\bar{\alpha}_M$ is also 12, and $F(\alpha_M/2) = F(2\alpha_M) = 0.01\ F(\alpha_M)$.

(Morel and Bricaud 1986)

Scattering phase function: Effects of particle size and refractive index

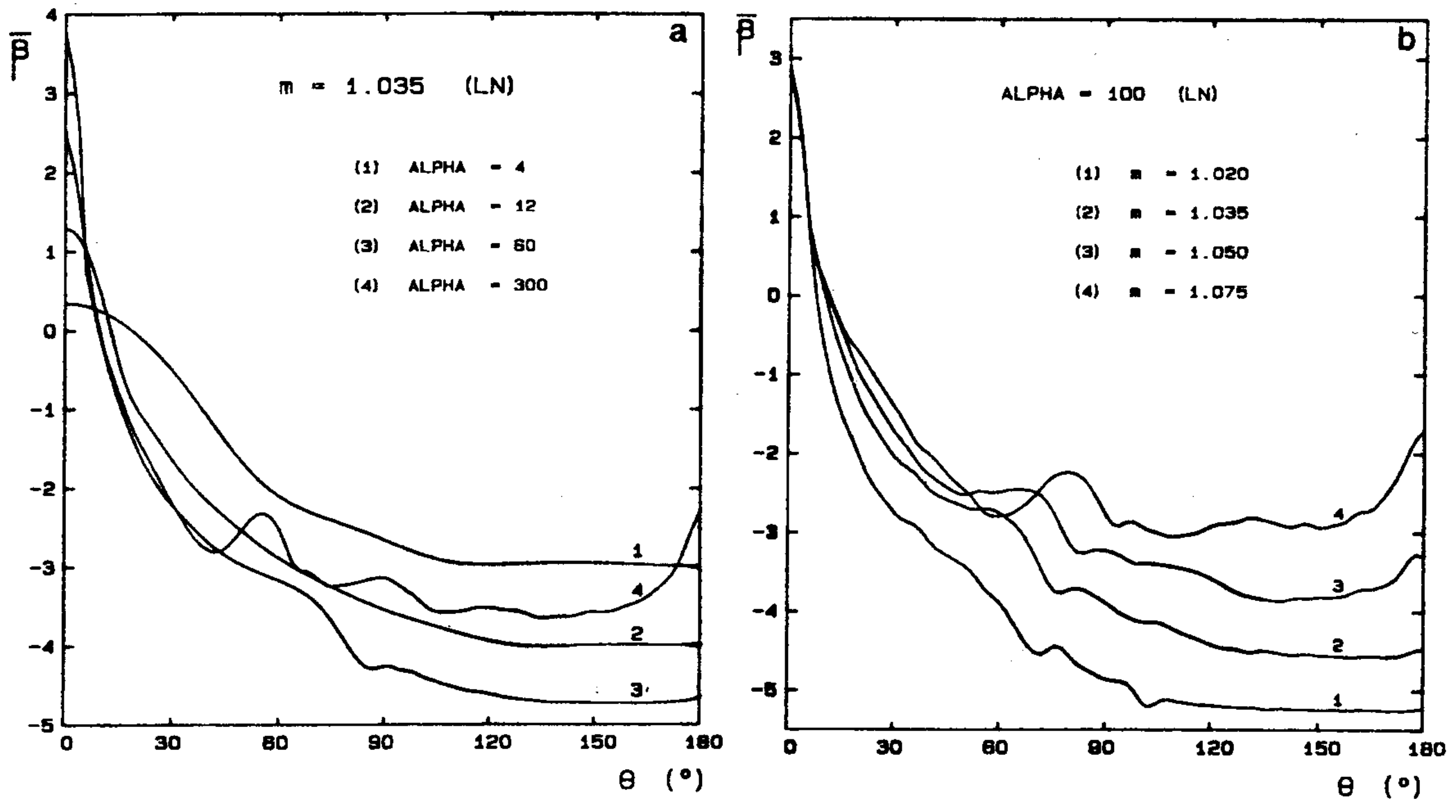

FIG. 6. (a) Normalized volume scattering function $\bar{\beta}(\theta)$ for increasing α_M values (increasing size) and for $m = 1.035$. (b) Normalized volume scattering function $\bar{\beta}(\theta)$ for increasing (real) index of refraction and for $\alpha_M = 100$. For Fig. 6a and b the log normal size distribution used is as in Fig. 5. The "bump" which occurs at about 75° for $m = 1.075$ and at smaller angles when the refractive index decreases (see also Fig. 6a) is the first "rainbow", at 138° for water droplets ($n = 1.33$). It appears for sufficiently large and perfect spheres. Thus it is unlikely that it can be observed for algal cells.

(Morel and Bricaud 1986)

Normalized scattering function for various microorganisms (from Mie calculations)

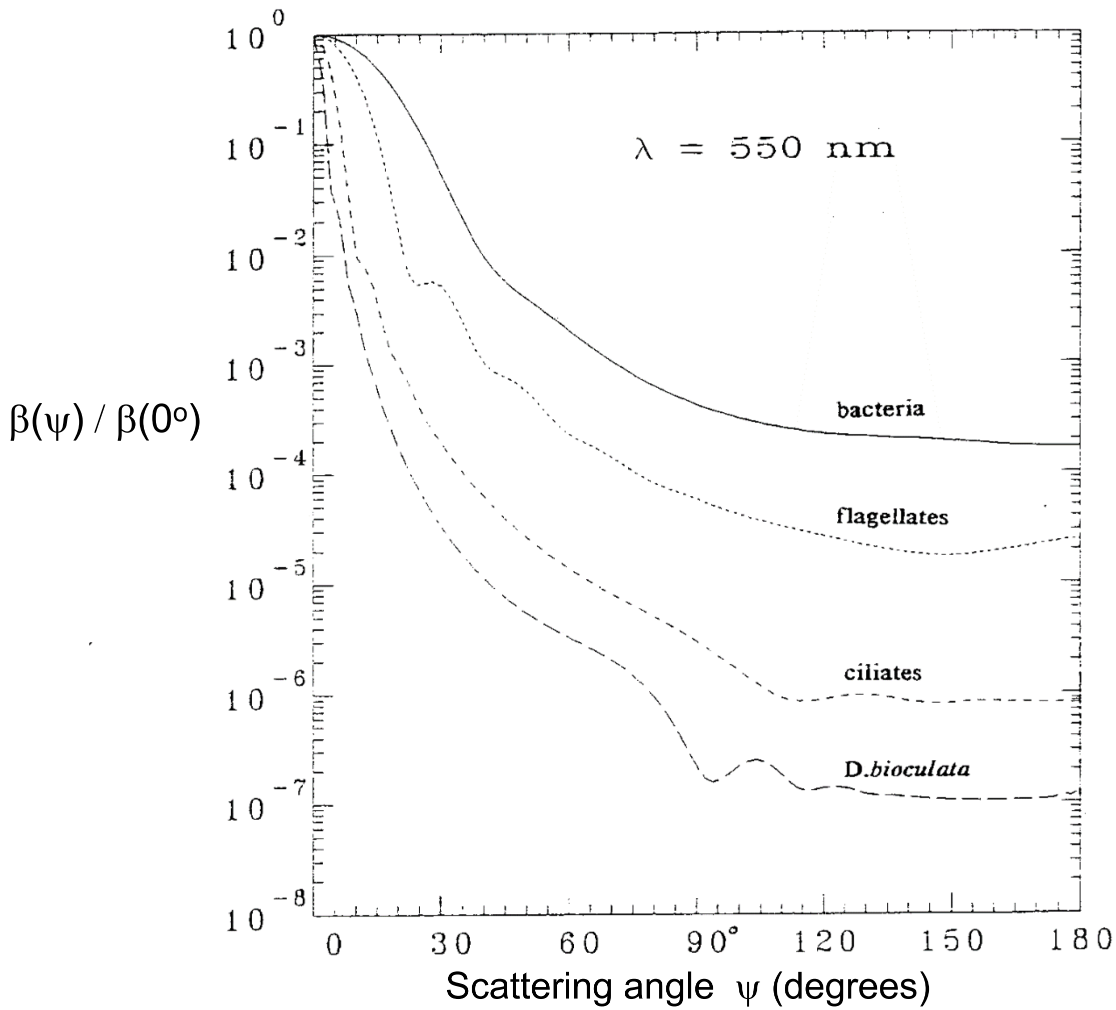

Figure 6. Volume scattering function (normalized at $\theta = 0°$ and for $\lambda = 550$ nm) computed for various organisms by using their refractive index and size distribution as experimentally determined (see text).

(Morel 1991)

Backscattering ratio versus particle size parameter

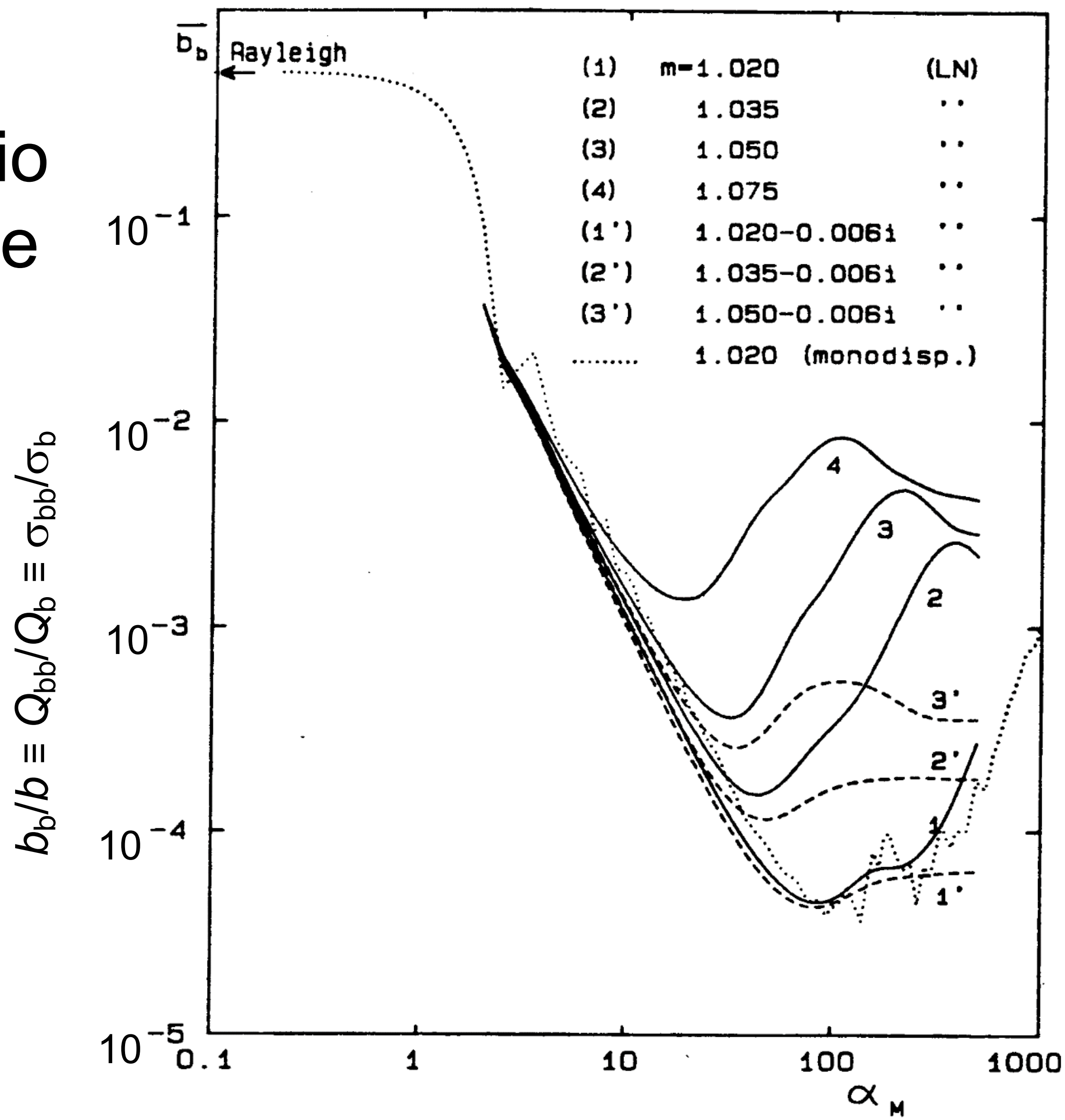

FIG. 8. Variations of the backscattering ratio $\bar{b}_b$ ($= b_b/b$) vs. the modal relative size α_M (same log-normal law as before in Fig. 5). The different curves correspond to various values of the refractive index given in inset. The curve for a monodispersed population (with $m = 1.02$) is also shown (dotted line). The arrow indicates the limiting value of b_b/b ($=0.5$) when α tends toward 0 (Rayleigh domain).

(Morel and Bricaud 1986)

INTERSPECIES OPTICAL VARIABILITY OF PLANKTON MICROORGANISMS

Particle size and complex refractive index are the first-order determinants of interspecies variability of single-particle optical properties

Plankton microorganisms

Table 1. Microbial components in the database and source of raw data. Values for the average equivalent spherical diameter (D), the real part of refractive index at 550 nm (n), and imaginary part of refractive index at 440 and 675 nm (n') are also given for each component.

i	Label	Microbial species	D [μm]	n 550 nm	$n' \cdot 10^3$ 440 nm	$n' \cdot 10^3$ 675 nm	Source of raw data
1	VIRU	Viruses	0.07	1.050	0	0	Stramski and Kiefer, 1991
2	HBAC	Heterotrophic bacteria	0.55	1.055	0.509	0.057	Stramski and Kiefer, 1990
3	PROC	generic Prochlorophyte; the average of:	0.66	1.051	18.51	10.30	
		PMED - Prochlorococcus strain MED	0.59	1.055	23.25	13.77	Morel et al., 1993
		PNAS - average of Prochlorococcus strains NATL and SARG	0.70	1.046	13.78	6.687	Morel et al., 1993
4	SYNE	generic Synechococcus; the average of:	1.05	1.051	5.587	2.930	
		SM41 - Synechococcus strain MAX41 (Cyanophyceae)	0.92	1.047	5.415	2.905	Morel et al., 1993
		SM01 - Synechococcus strain MAX01 (Cyanophyceae)	0.94	1.049	4.505	2.547	Morel et al., 1993
		SROS - Synechococcus strain ROS04 (Cyanophyceae)	1.08	1.049	4.516	2.154	Morel et al., 1993
		SDC2 - Synechococcus strain DC2 (Cyanophyceae)	1.14	1.050	4.249	2.375	Morel et al., 1993
		S103 - Synechococcus strain WH8103 (Cyanophyceae)	1.14	1.062	9.251	4.668	Stramski et al., 1995
5	SYMA	generic phycocyanin-rich picophytoplankton; the average of:	1.41	1.055	6.495	2.757	
		SCYS - Synechocystis (Cyanophyceae)	1.39	1.050	4.530	1.910	Ahn et al., 1992
		MARI - Anacystis marina (Cyanophyceae)	1.43	1.060	8.460	3.603	Ahn et al., 1992
6	PING	Pavlova pinguis (Haptophyceae)	3.97	1.046	4.177	2.709	Bricaud et al., 1988
7	PSEU	Thalassiosira pseudonana (Bacillariophyceae)	3.99	1.045	9.231	7.397	Stramski and Reynolds, 1993
8	LUTH	Pavlova lutheri (Haptophyceae)	4.26	1.045	5.767	2.403	Bricaud et al., 1988
9	GALB	Isochrysis galbana (Haptophyceae)	4.45	1.056	7.673	5.101	Ahn et al., 1992
10	HUXL	Emiliania huxleyi (Haptophyceae)	4.93	1.050	5.012	2.950	Ahn et al., 1992
11	CRUE	Porphyridium cruentum (Rhodophyceae)	5.22	1.051	3.351	2.443	Bricaud et al., 1988
12	FRAG	Chroomonas fragarioides (Cryptophyceae)	5.57	1.039	4.275	2.904	Ahn et al., 1993
13	PARV	Prymnesium parvum (Haptophyceae)	6.41	1.045	2.158	1.329	Bricaud et al., 1988
14	BIOC	Dunaliella bioculata (Chlorophyceae)	6.71	1.038	10.49	7.839	Ahn et al., 1993
15	TERT	Dunaliella tertiolecta (Chlorophyceae)	7.59	1.063	6.260	5.076	Stramski et al., 1993
16	CURV	Chaetoceros curvisetum (Bacillariophyceae)	7.73	1.024	2.877	1.480	Bricaud et al., 1988
17	ELON	Hymenomonas elongata (Haptophyceae)	11.77	1.046	13.87	7.591	Ahn et al., 1992
18	MICA	Prorocentrum micans (Dinophyceae)	27.64	1.045	2.466	1.710	Ahn et al., 1992

(Stramski et al. 2001)

Interspecies variability of absorption properties

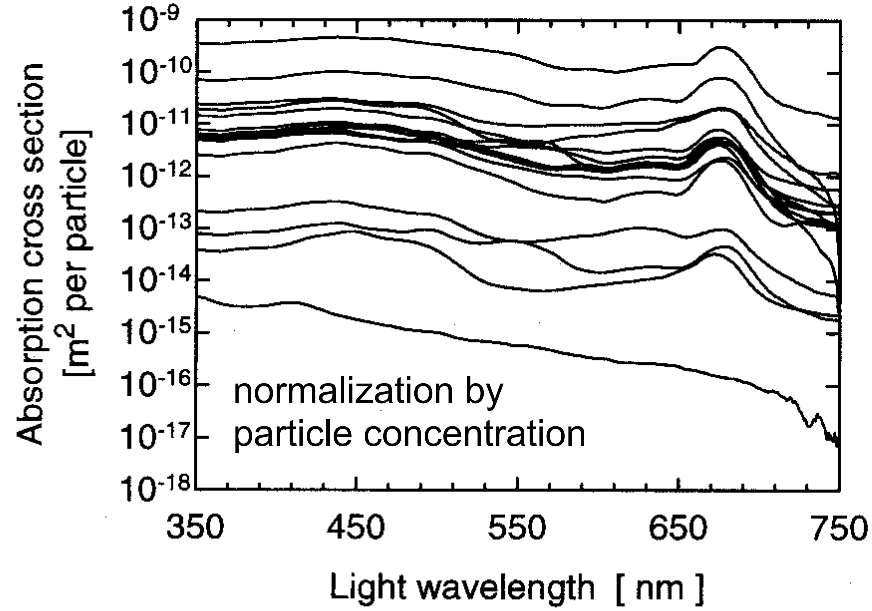

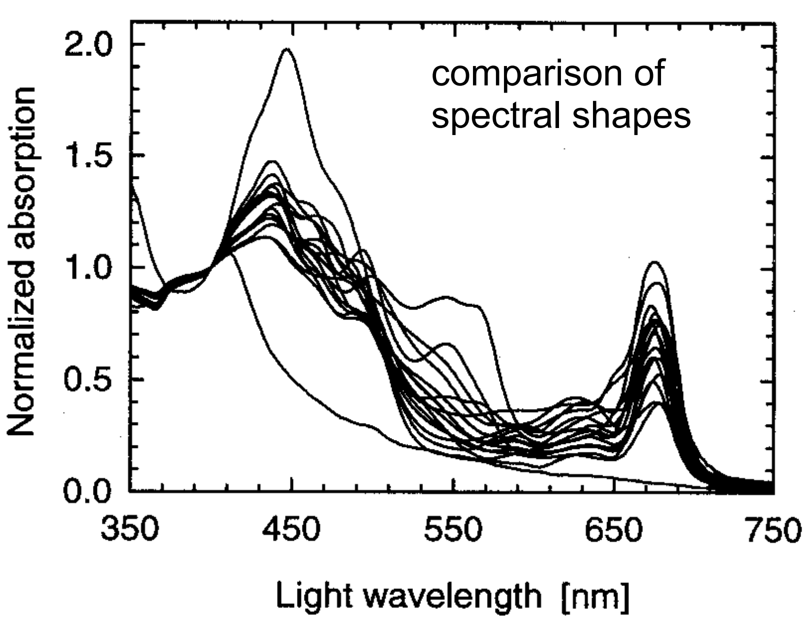

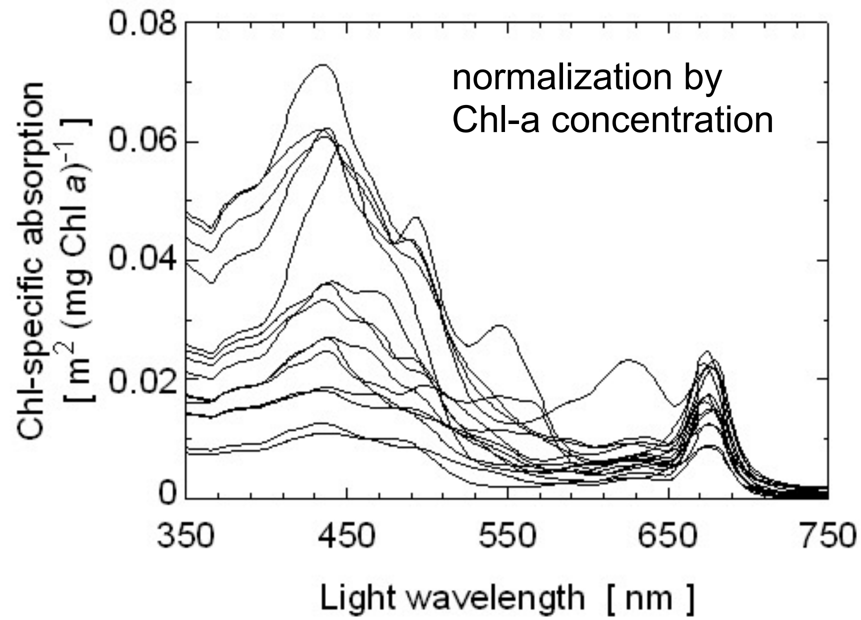

(Stramski et al. 2001)

Interspecies variability of scattering properties

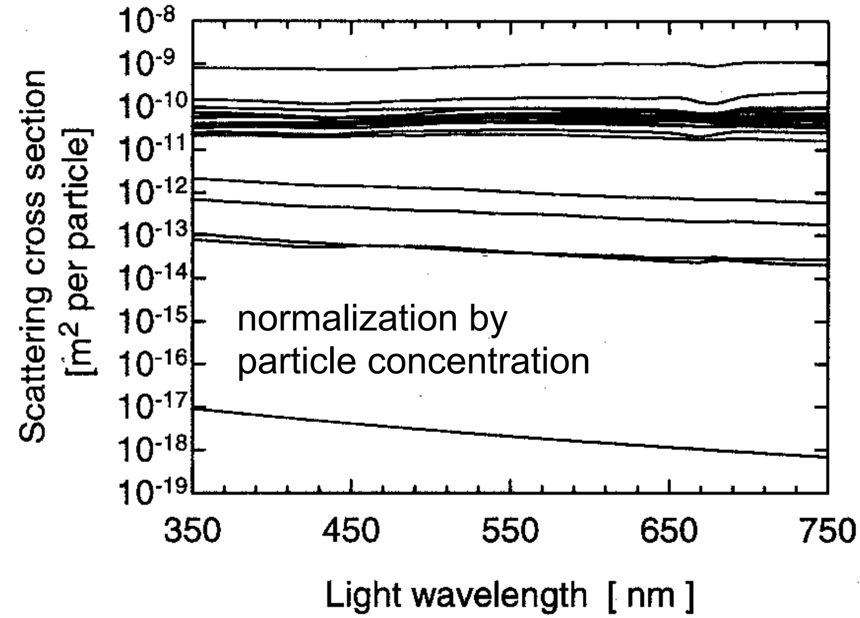

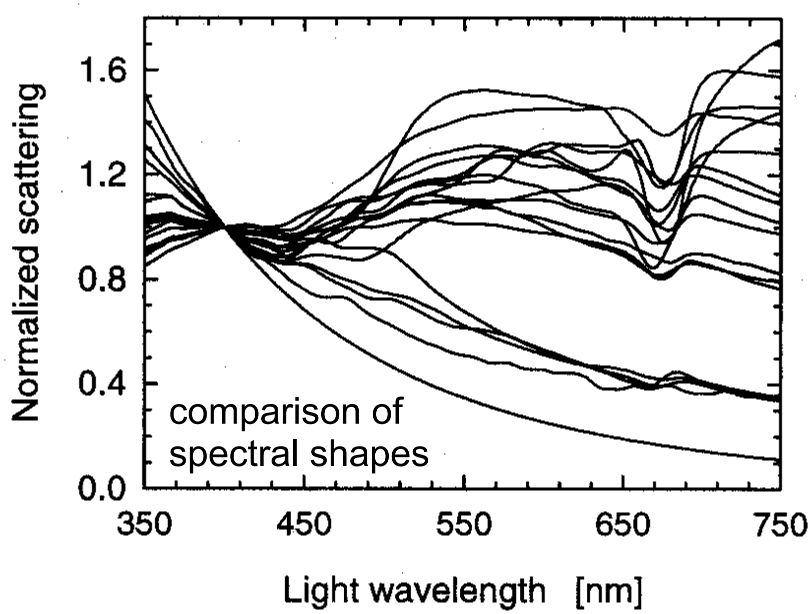

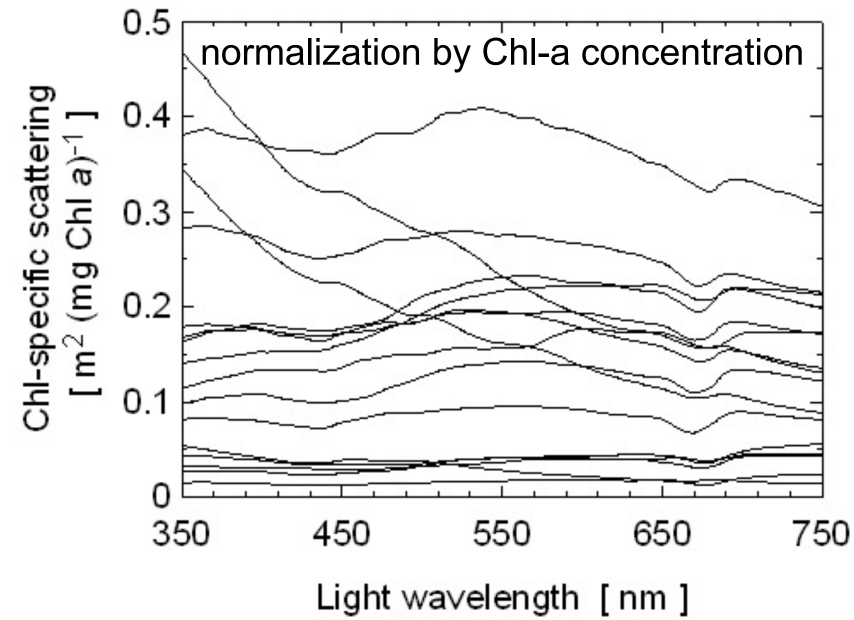

(Stramski et al. 2001)

Mie calculations of scattering phase function for plankton microorganisms

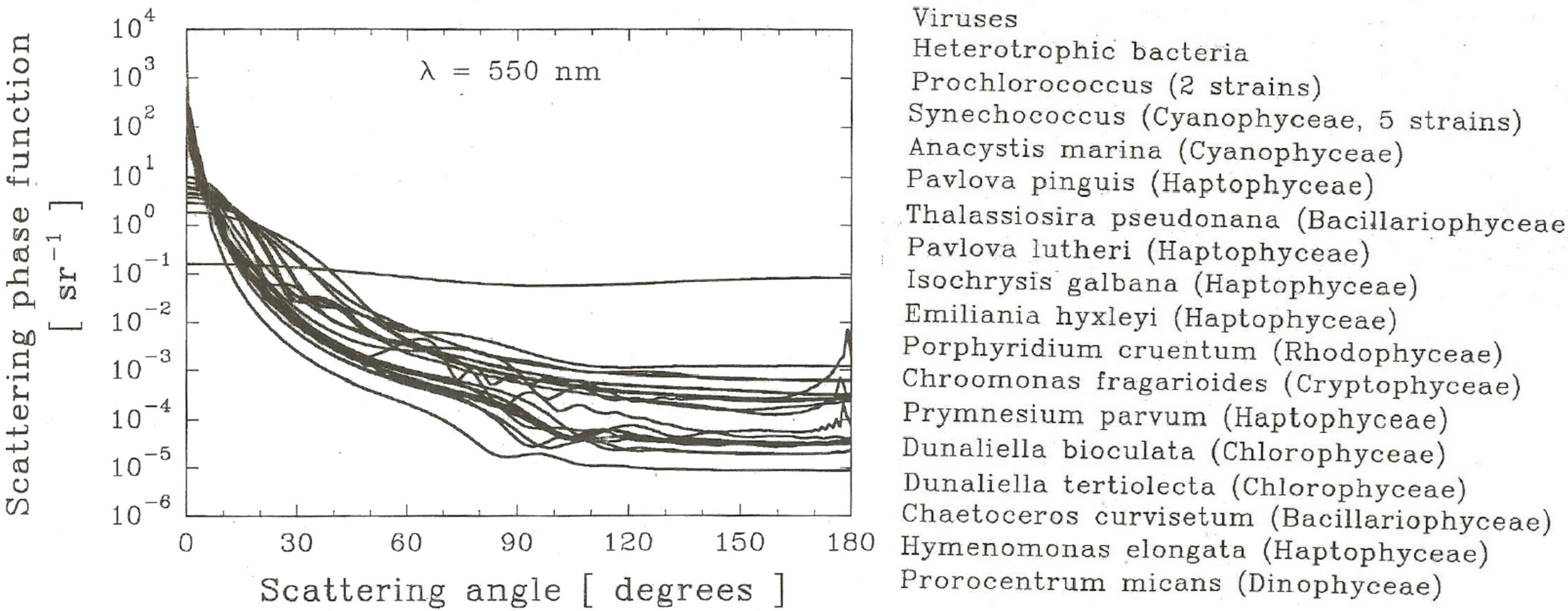

(Stramski et al. 2001)

INTRASPECIES OPTICAL VARIABILITY OF PLANKTON MICROORGANISMS

Plankton optical properties vary in response to varying growth conditions:
light, nutrients, temperature

Intraspecies variability due to acclimation to growth irradiance cyanobacteria *Synechocystis*

Absorption

Scattering

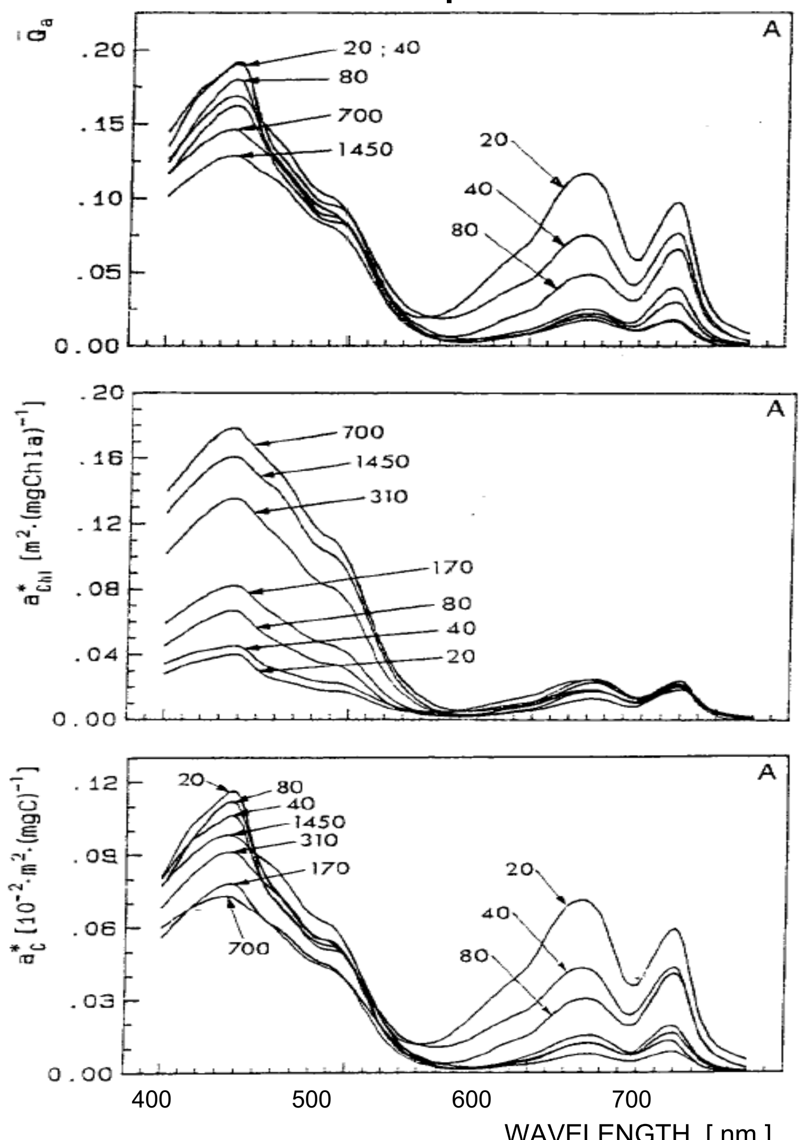

Optical efficiency

Chla-specific

Carbon-specific

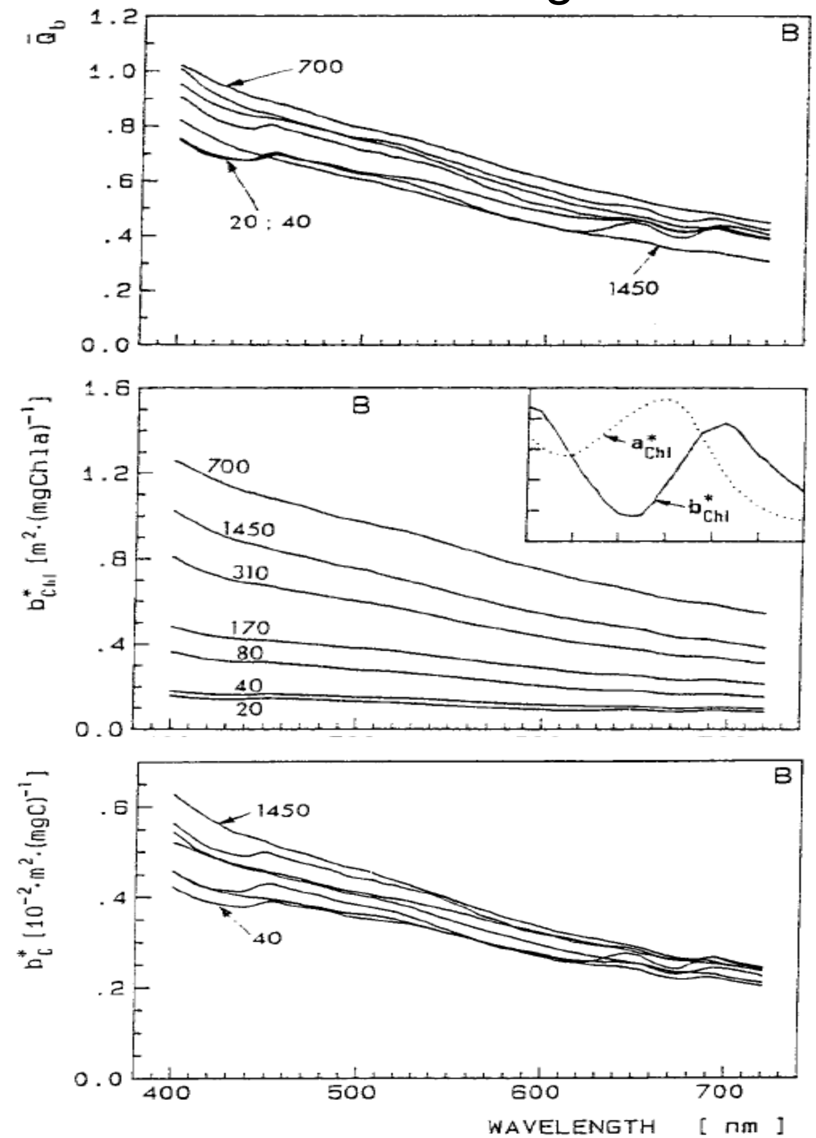

(Stramski and Morel 1990)

Intraspecies variability over a diel cycle

diatom
Thalassiosira pseudonana

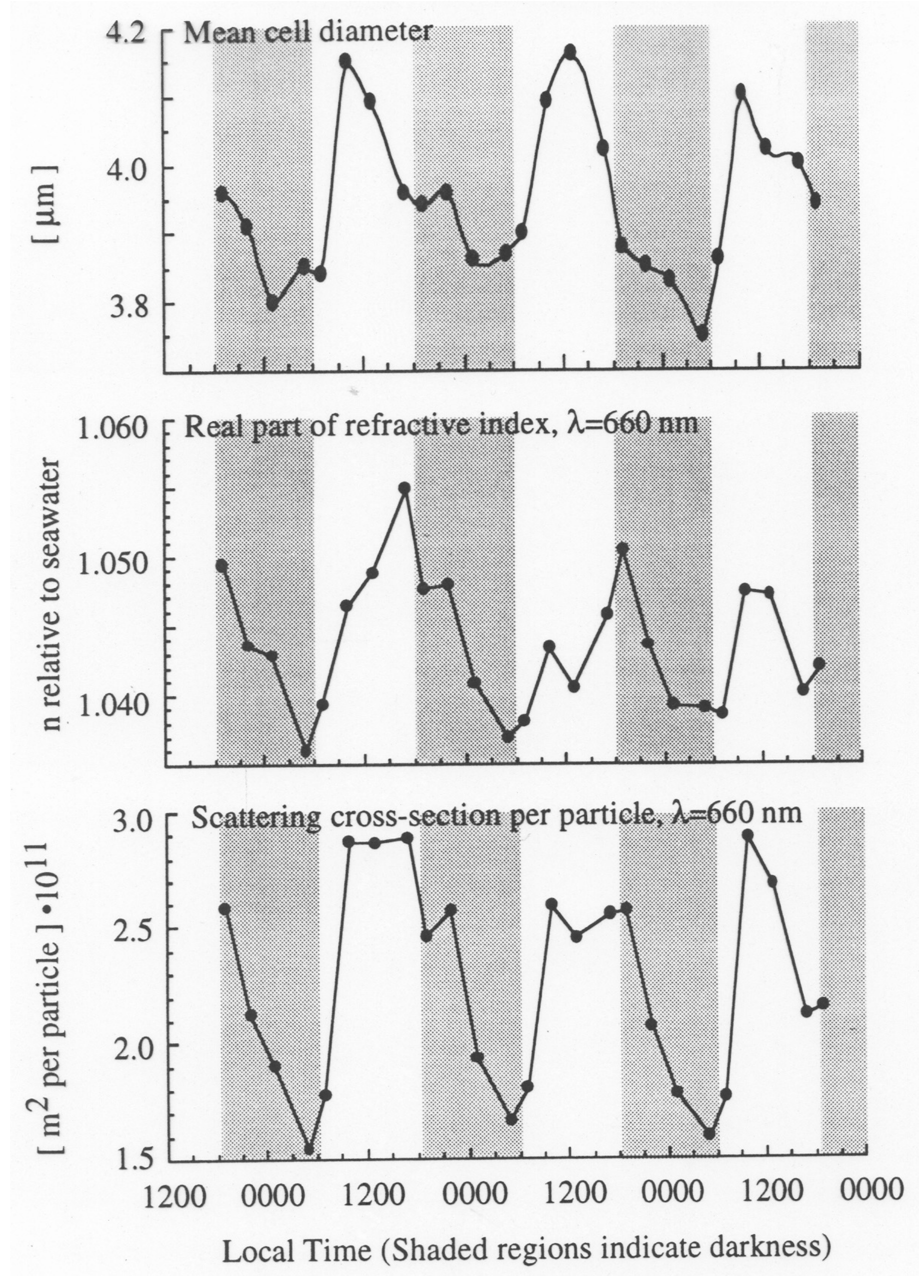

(Stramski and Reynolds 1993)

Optical properties of heterotrophic bacteria

Absorption

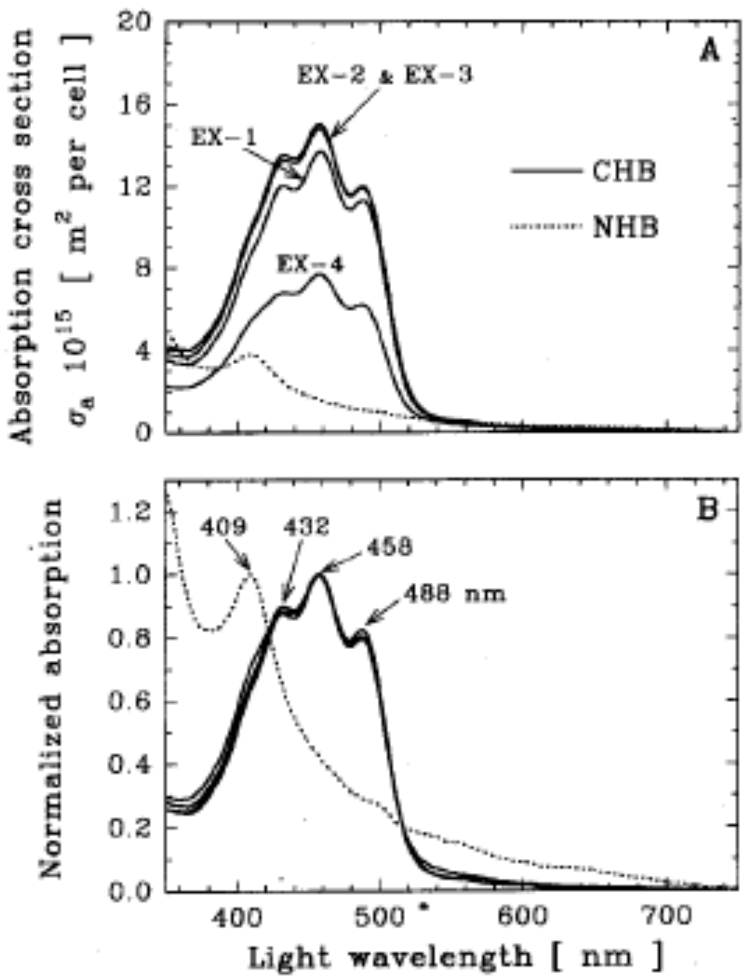

Beam attenuation

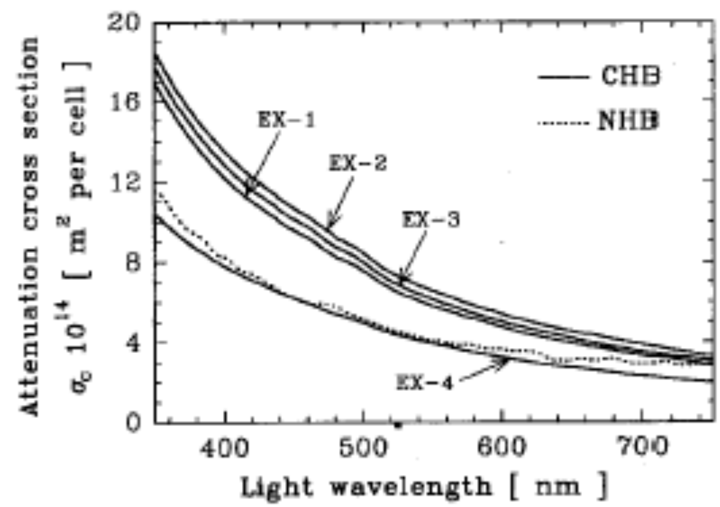

CHB Carotenoid-rich bacteria:
grown in nutrient-enriched seawater [EX-1 (light-dark cycle), EX-2 and EX-3 (dark)], and in nutrient-poor seawater (EX-4)

NHB Non-pigmented bacteria:
fast-growing in the absorption experiment and starved in the attenuation experiment

(Stramski and Kiefer 1998)

Absorption of mineral-rich particulate assemblages

Mass-specific absorption

(normalization by mass concentration of particles)

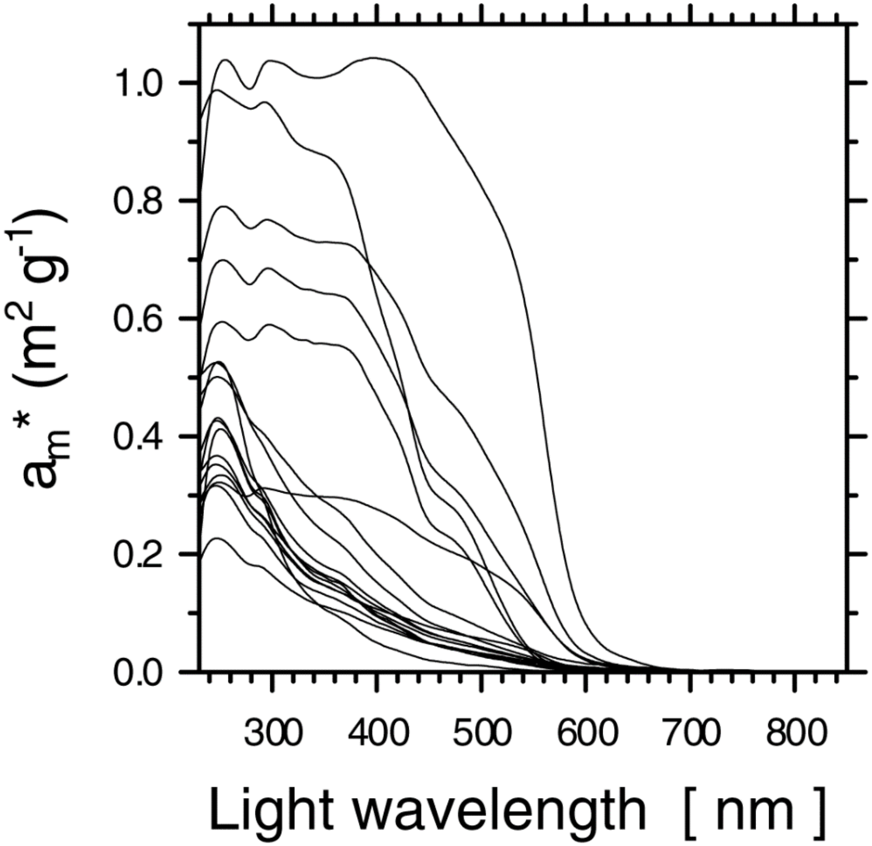

Fe-specific absorption

(normalization by mass concentration of iron)

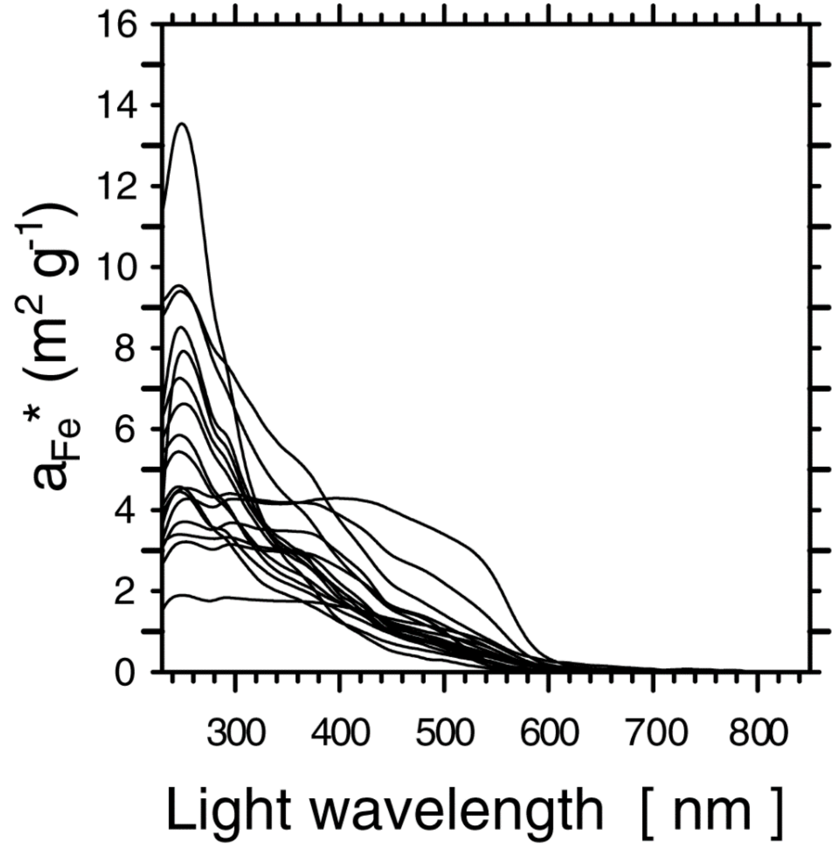

(Babin and Stramski 2004)

(Babin and Stramski 2004)

Terrigenous mineral-rich particulate matter

Sample ID	Description	Origin
ILL_1	illite	Source Clay Minerals Repository, University of Missouri (ref. IMt-1)
ILL_2	as above but different PSD	as above
KAO_1	kaolinite (poorly crystallized)	as above (ref. KGa-2)
KAO_2	as above but different PSD	as above
MON_1	Ca-montmorillonite	as above (ref. SAz-1)
MON_2	as above but different PSD	as above
CAL_1	calcite	natural crystal
CAL_2	as above but different PSD	as above
QUA_1	quartz	natural crystal
SAH_1	atmospheric dust from Sahara	red rain event, Villefranche-sur-Mer, France
SAH_2	as above but different PSD	as above
AUS_1	surface soil dust	cliff shore, Palm Beach near Sydney, Australia
AUS_2	as above but different PSD	as above
ICE_1	ice-rafted particles	glacier runoff, Kongsfjord, Spitsbergen
ICE_2	as above but different PSD	as above
OAH_1	surface soil dust	Oahu, Hawaii Islands
OAH_2	as above but different PSD	as above
KUW_1	surface soil dust	Kuwait (eastern part, close to ocean)
KUW_2	as above but different PSD	as above
NIG_1	surface soil dust	southwest Nigeria
SAN_1	atmospheric dust	San Diego, California

(Stramski et al. 2007)

Mass-specific absorption

Mass-specific scattering

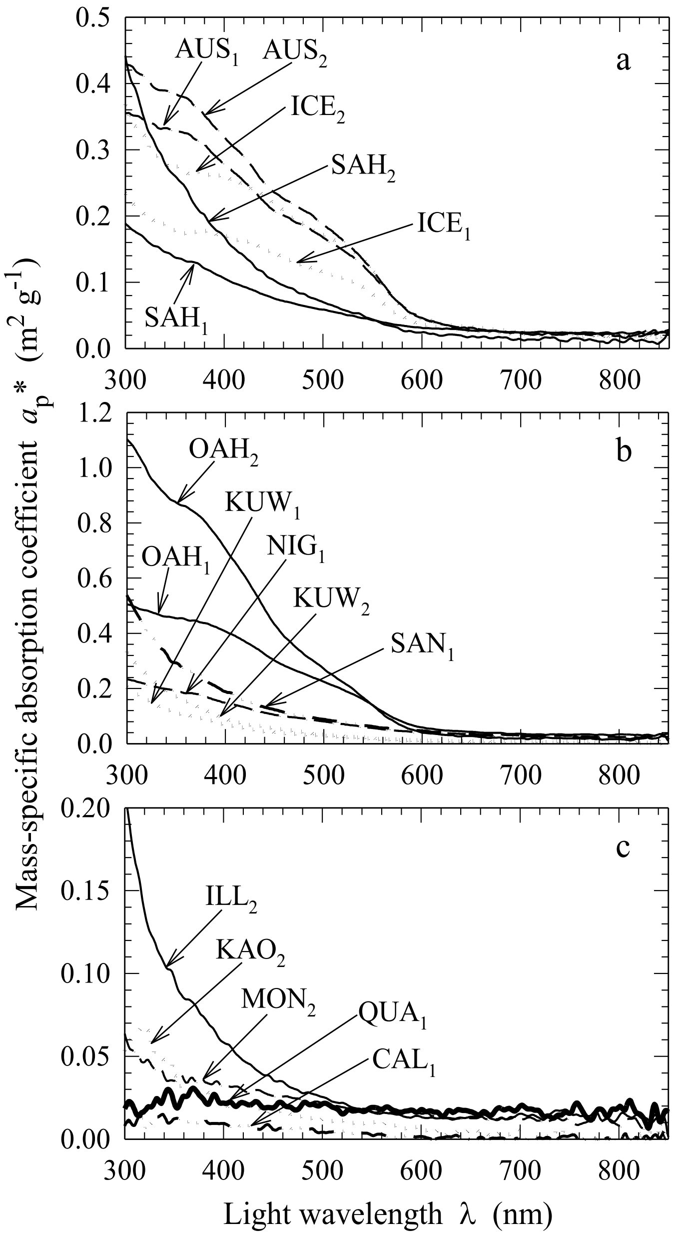

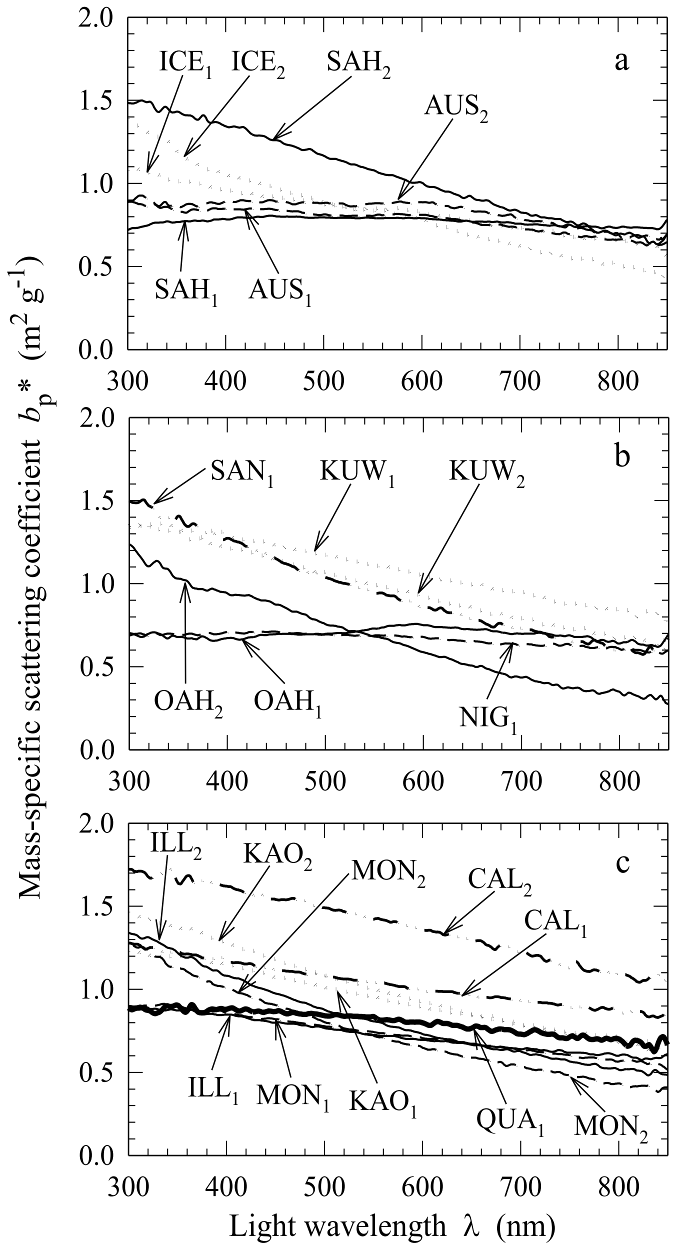

(Stramski et al. 2007)

Colloidal particles (<1 μm in size) – Particle size distributions

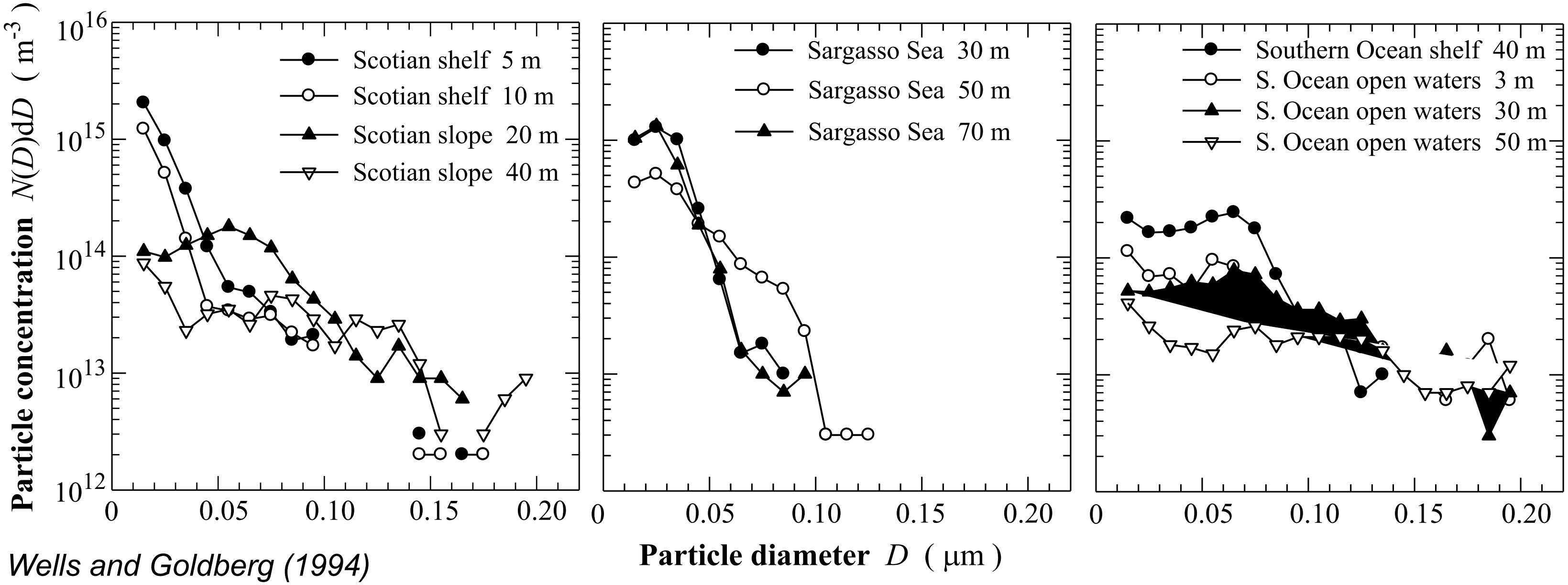

Wells and Goldberg (1994)

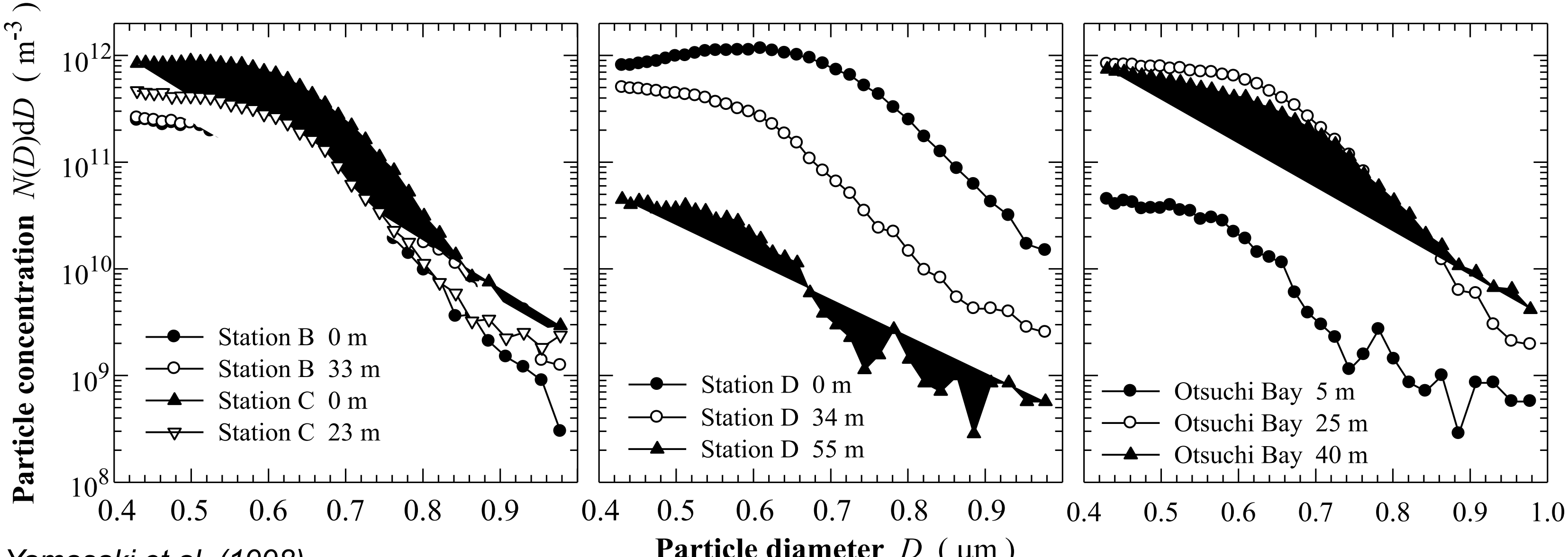

Yamasaki et al. (1998)

Assessment of scattering and backscattering coefficients of colloidal particles: Comparison with pure seawater

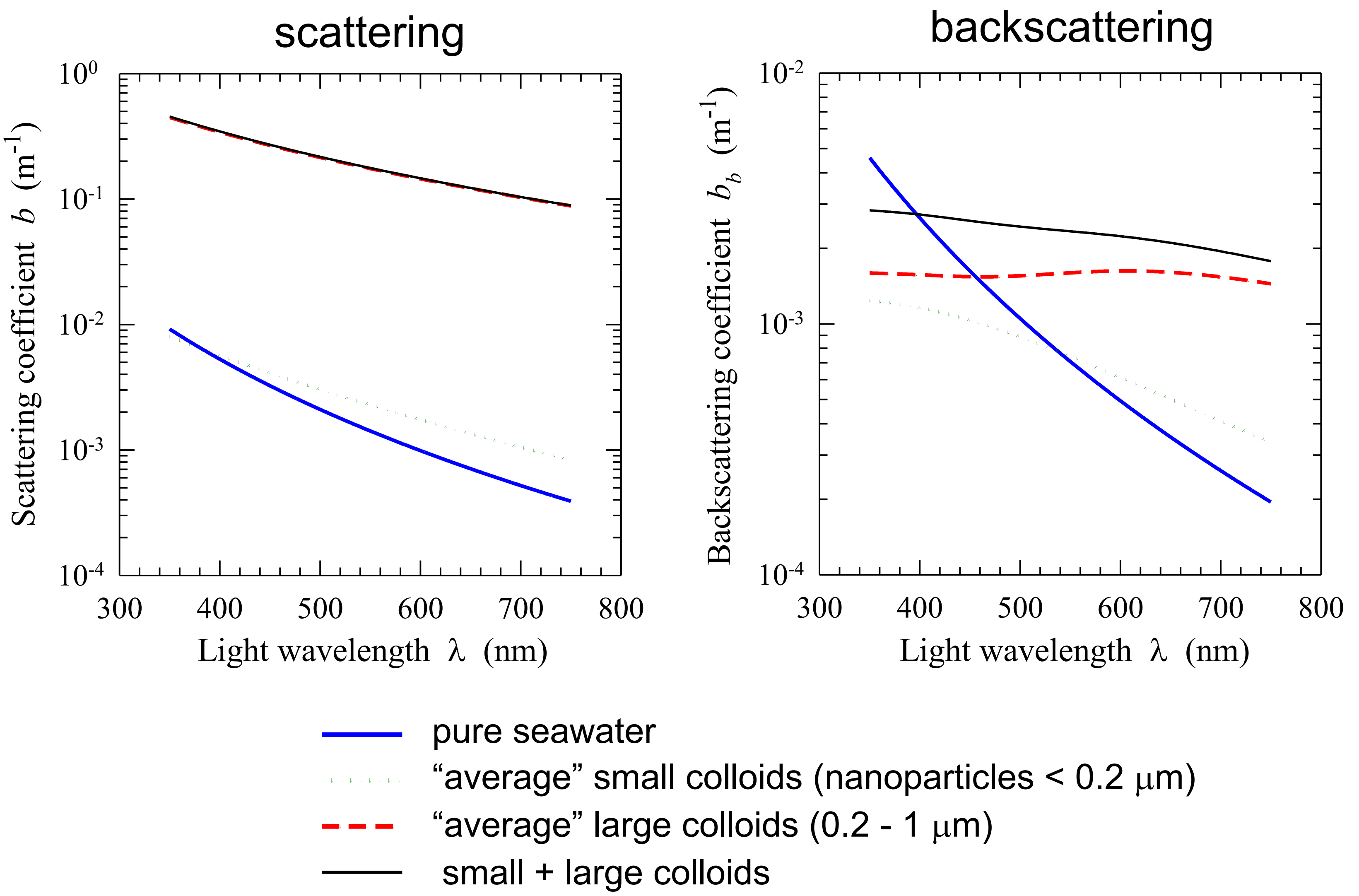

(Stramski and Woźniak 2005)

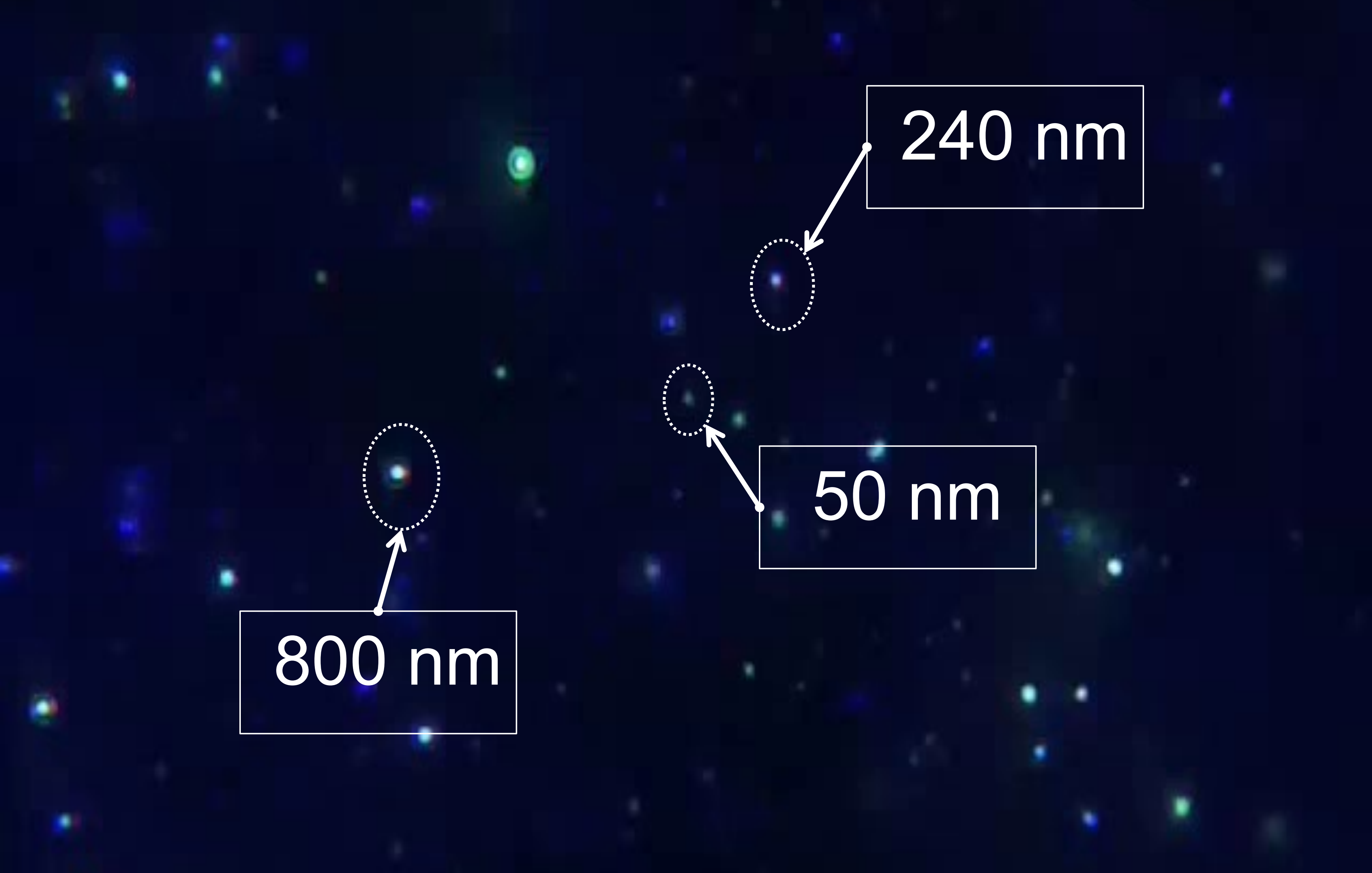

Measurement of a wide range of nanoparticle sizes simultaneously using novel MANTA technology (Multispectral Advanced Nanoparticle Tracking Analysis)

A superposition of 300 video frames acquired during 10 seconds illustrating trajectories of individual nanoparticles through time

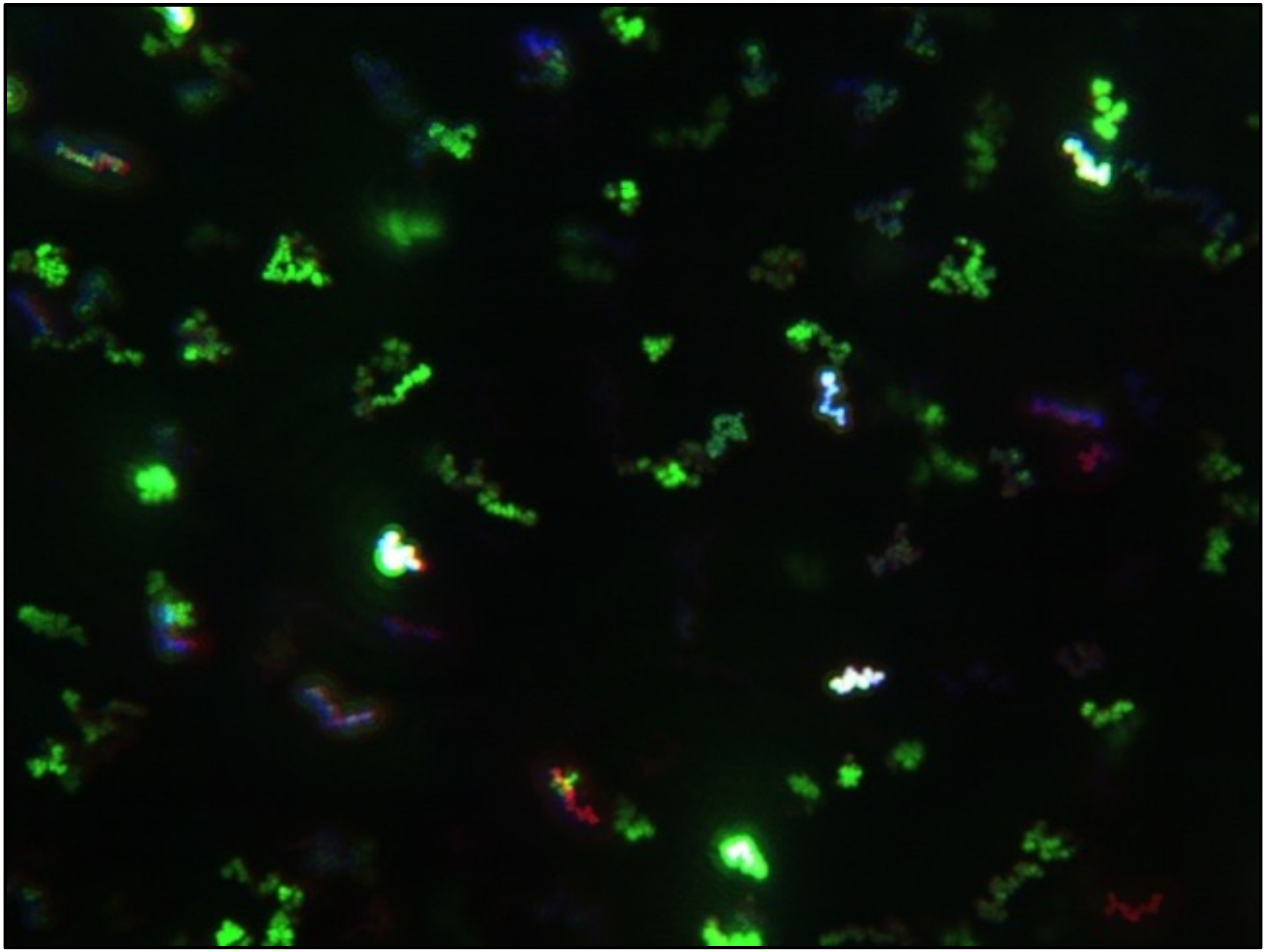

A mix of polystyrene nanosphere size standards of 50, 240, and 800 nm in diameter suspended in water

1905 Albert Einstein's Year of Miracles: One of four "Annus Mirabilis" papers:

5. *Über die von der molekularkinetischen Theorie der Wärme geforderte Bewegung von in ruhenden Flüssigkeiten suspendierten Teilchen;* von A. Einstein.

In dieser Arbeit soll gezeigt werden, daß nach der molekularkinetischen Theorie der Wärme in Flüssigkeiten suspendierte Körper von mikroskopisch sichtbarer Größe infolge der Molekularbewegung der Wärme Bewegungen von solcher Größe ausführen müssen, daß diese Bewegungen leicht mit dem Mikroskop nachgewiesen werden können. Es ist möglich, daß die hier zu behandelnden Bewegungen mit der sogenannten „Brownschen Molekularbewegung" identisch sind; die mir erreichbaren Angaben über letztere sind jedoch so ungenau, daß ich mir hierüber kein Urteil bilden konnte.

Wenn sich die hier zu behandelnde Bewegung samt den für sie zu erwartenden Gesetzmäßigkeiten wirklich beobachten läßt, so ist die klassische Thermodynamik schon für mikroskopisch unterscheidbare Räume nicht mehr als genau gültig anzusehen und es ist dann eine exakte Bestimmung der wahren Atomgröße möglich. Erwiese sich umgekehrt die Voraussage dieser Bewegung als unzutreffend, so wäre damit ein schwerwiegendes Argument gegen die molekularkinetische Auffassung der Wärme gegeben.

§ 1. Über den suspendierten Teilchen zuzuschreibenden osmotischen Druck.

Im Teilvolumen V^* einer Flüssigkeit vom Gesamtvolumen V seien z-Gramm-Moleküle eines Nichtelektrolyten gelöst. Ist das Volumen V^* durch eine für das Lösungsmittel, nicht aber für die gelöste Substanz durchlässige Wand vom reinen Lösungs-

ON THE MOVEMENT OF SMALL PARTICLES SUSPENDED IN STATIONARY LIQUIDS REQUIRED BY THE MOLECULAR-KINETIC THEORY OF HEAT

by A. Einstein

[*Annalen der Physik* 17 (1905): 549-560]

It will be shown in this paper that, according to the molecular-kinetic theory of heat, bodies of microscopically visible size suspended in liquids must, as a result of thermal molecular motions, perform motions of such magnitude that these motions can easily be detected by a microscope. It is possible that the motions to be discussed here are identical with the so-called "Brownian molecular motion"; however, the data available to me on the latter are so imprecise that I could not form a definite opinion on this matter.

If it is really possible to observe the motion to be discussed here, along with the laws it is expected to obey, then classical thermodynamics can no longer be viewed as strictly valid even for microscopically distinguishable spaces, and an exact determination of the real size of atoms becomes possible. Conversely, if the prediction of this motion were to be proved wrong, this fact would provide a weighty argument against the molecular-kinetic conception of heat.

$$D = \frac{k_B T}{3 \pi \eta D_{diff}}$$

D – diameter of particle

D_{diff} – diffusion coefficient of particle

T – temperature of the liquid medium (seawater)

η – dynamic viscosity of the medium (seawater)

k_B - Boltzmann constant

Scattering budget in terms of particle size fractions

Low-index particles

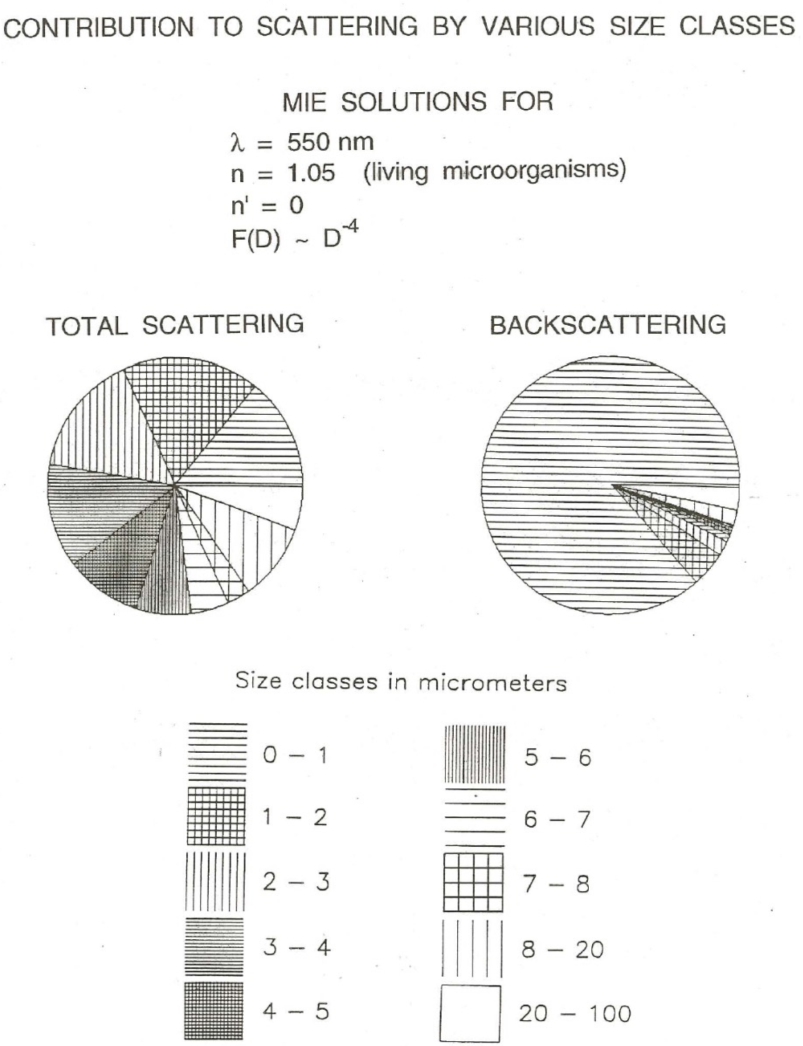

High-index particles

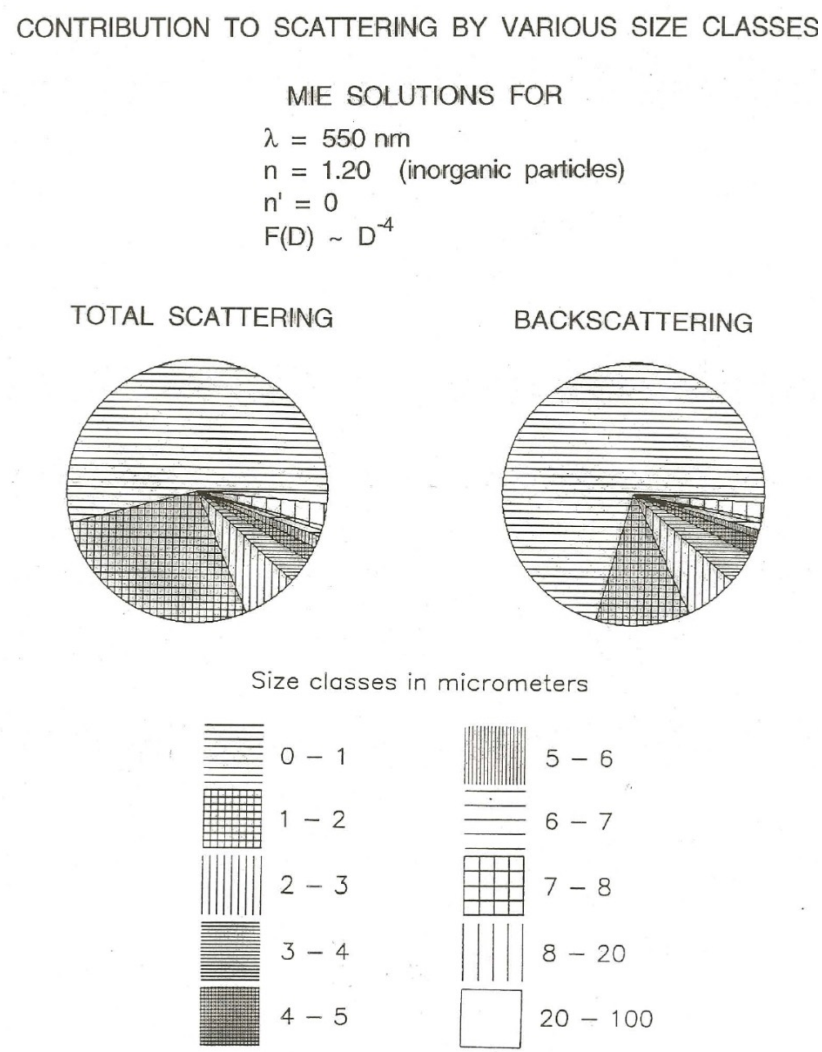

(Stramski and Kiefer 1991)

Light scattering by bubbles entrained by wave breaking

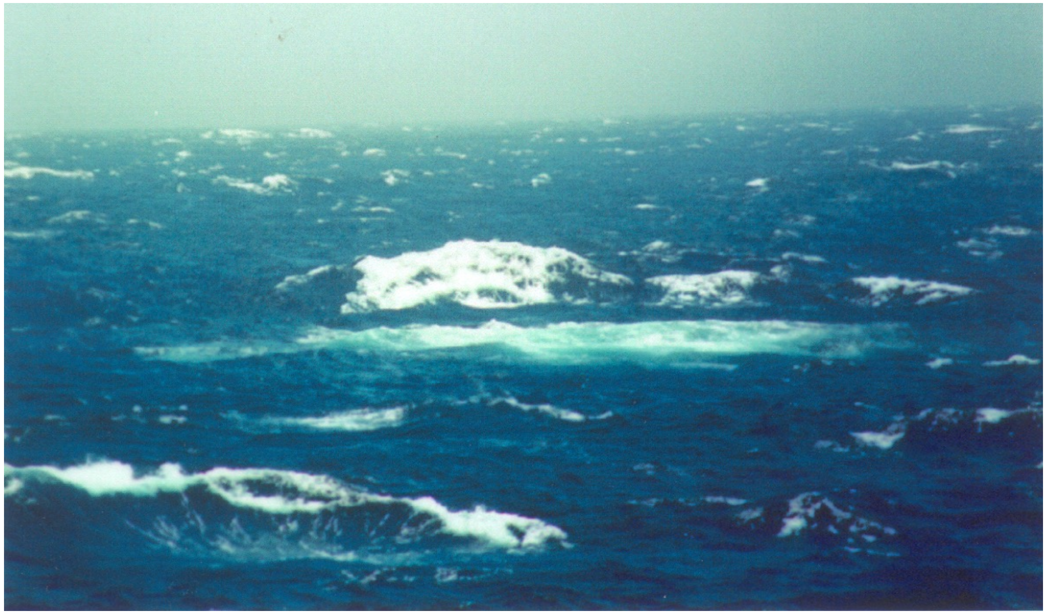

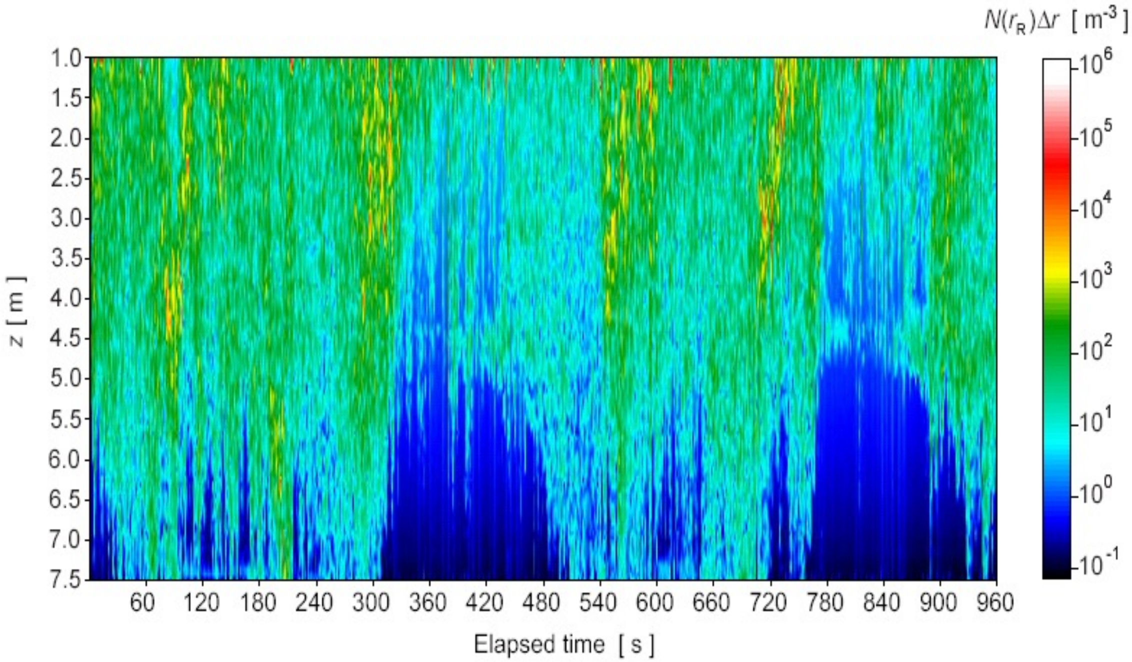

(Stramski and Tęgowski 2001)

Scattering and backscattering by bubbles as a function of void fraction

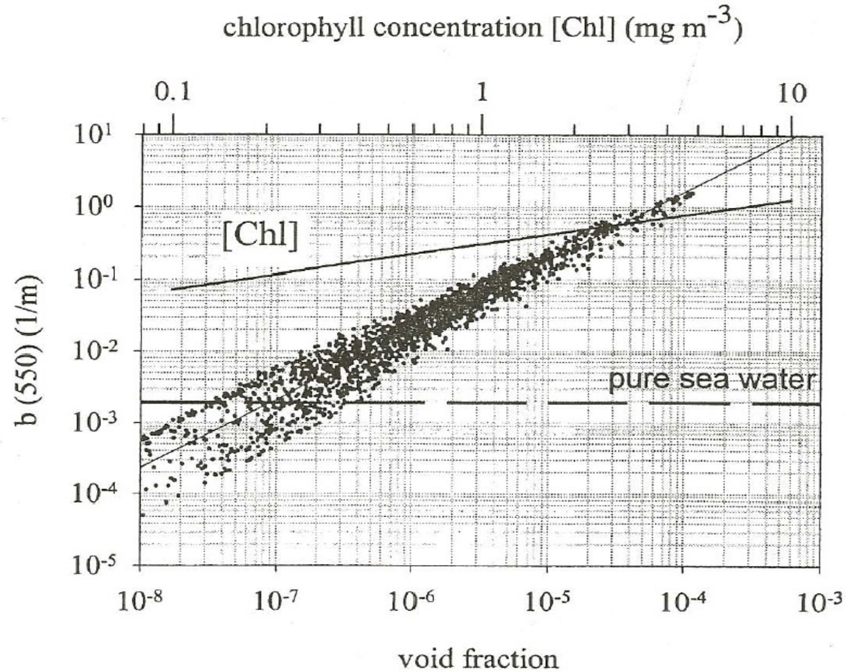

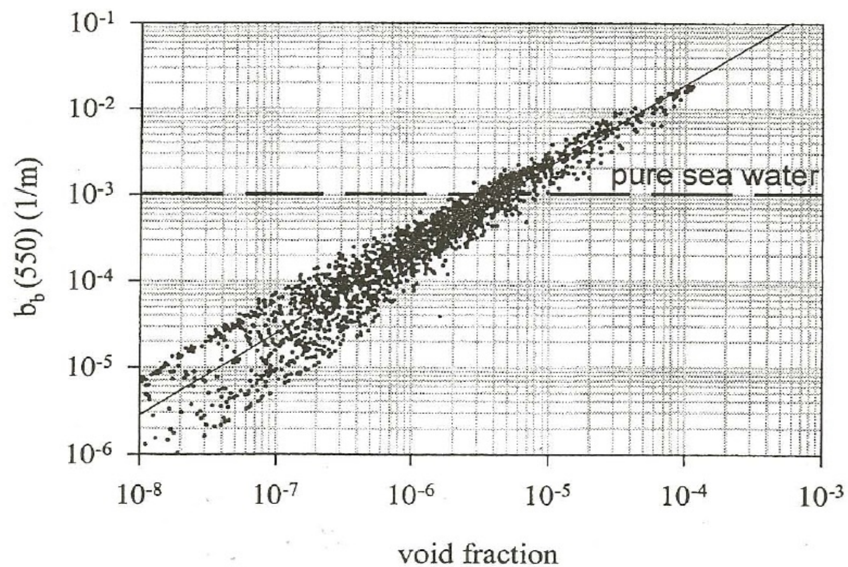

(Terrill et al. 2001)

Traditional approach with a few IOP components

Inherent Optical Properties (IOPs) are described in terms of a few broadly-defined categories of seawater constituents amenable to measurements

$$IOP(\lambda) = IOP_{w}(\lambda) + IOP_{p}(\lambda) + IOP_{CDOM}(\lambda)$$

$$IOP_{p}(\lambda) = IOP_{ph}(\lambda) + IOP_{NAP}(\lambda)$$

pure water (w), all particles (p), phytoplankton (ph), non-algal/detrital particles (NAP or d), chromophoric dissolved organic matter (CDOM or g)

Basic IOPs: absorption, scattering, and beam attenuation coefficients, volume scattering function

Four-component model of light absorption by seawater:

pure water (w), phytoplankton (ph), non-algal/detrital particles (d), and CDOM (g)

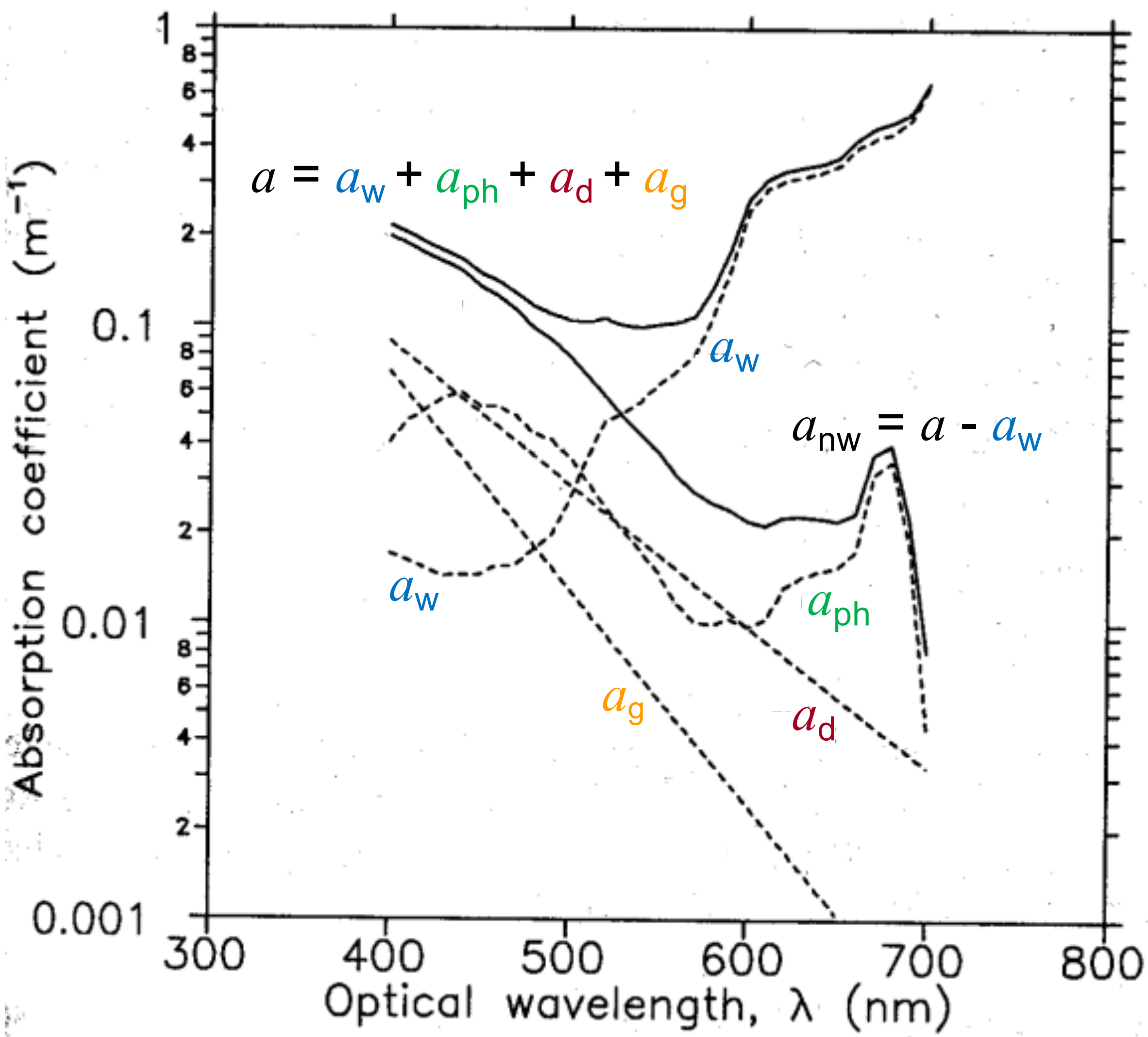

Examples of particulate absorption coefficients

a_p, a_d, a_{ph} (data from the Sargasso Sea)

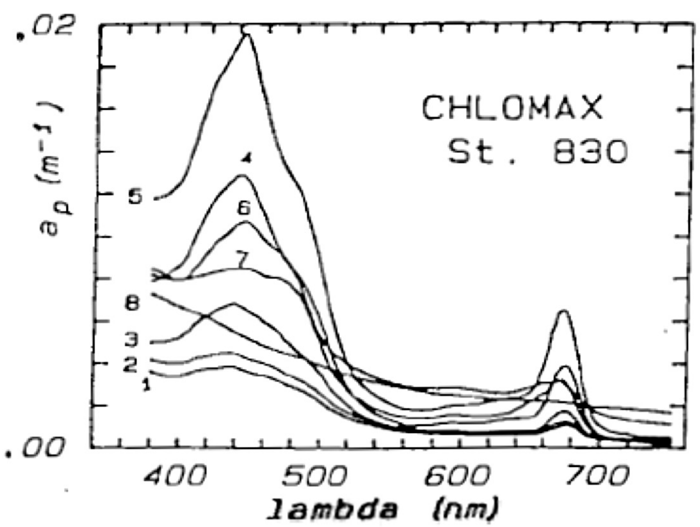

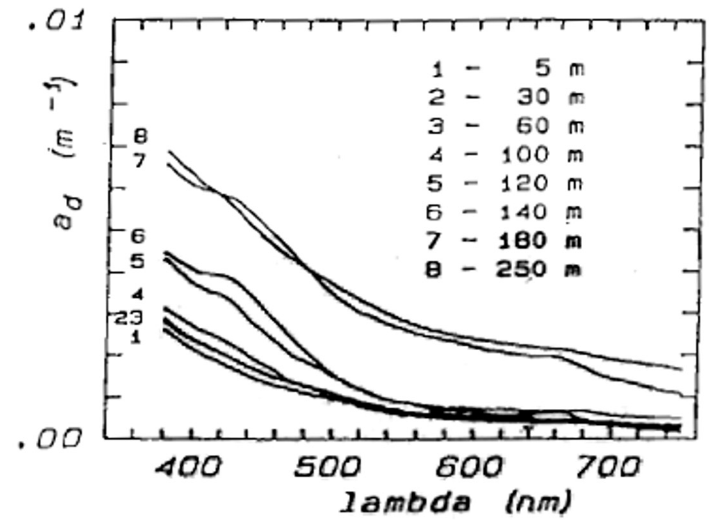

$$a_{ph} = a_p - a_d$$

$a_d \equiv a_{NAP}$ is the non-algal particulate absorption (more specifically, non-extractable in organic solvent or non-bleachable fraction of particulate absorption)

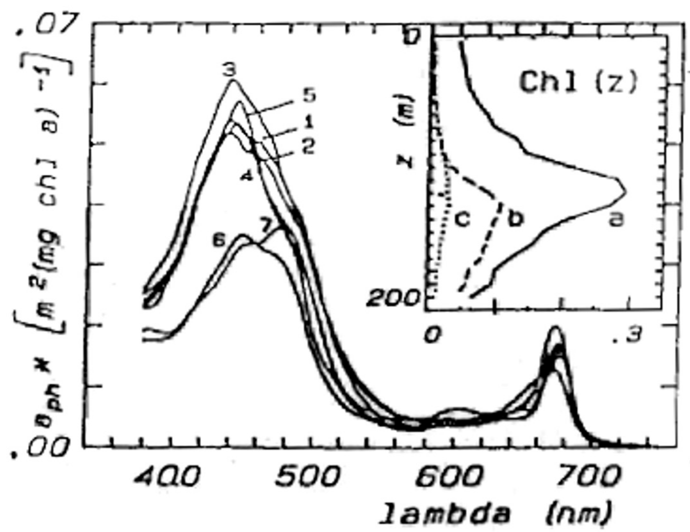

(Bricaud and Stramski 1990)

Example non-algal particulate (NAP) absorption spectra and the corresponding exponential fits based on data from different marine environments

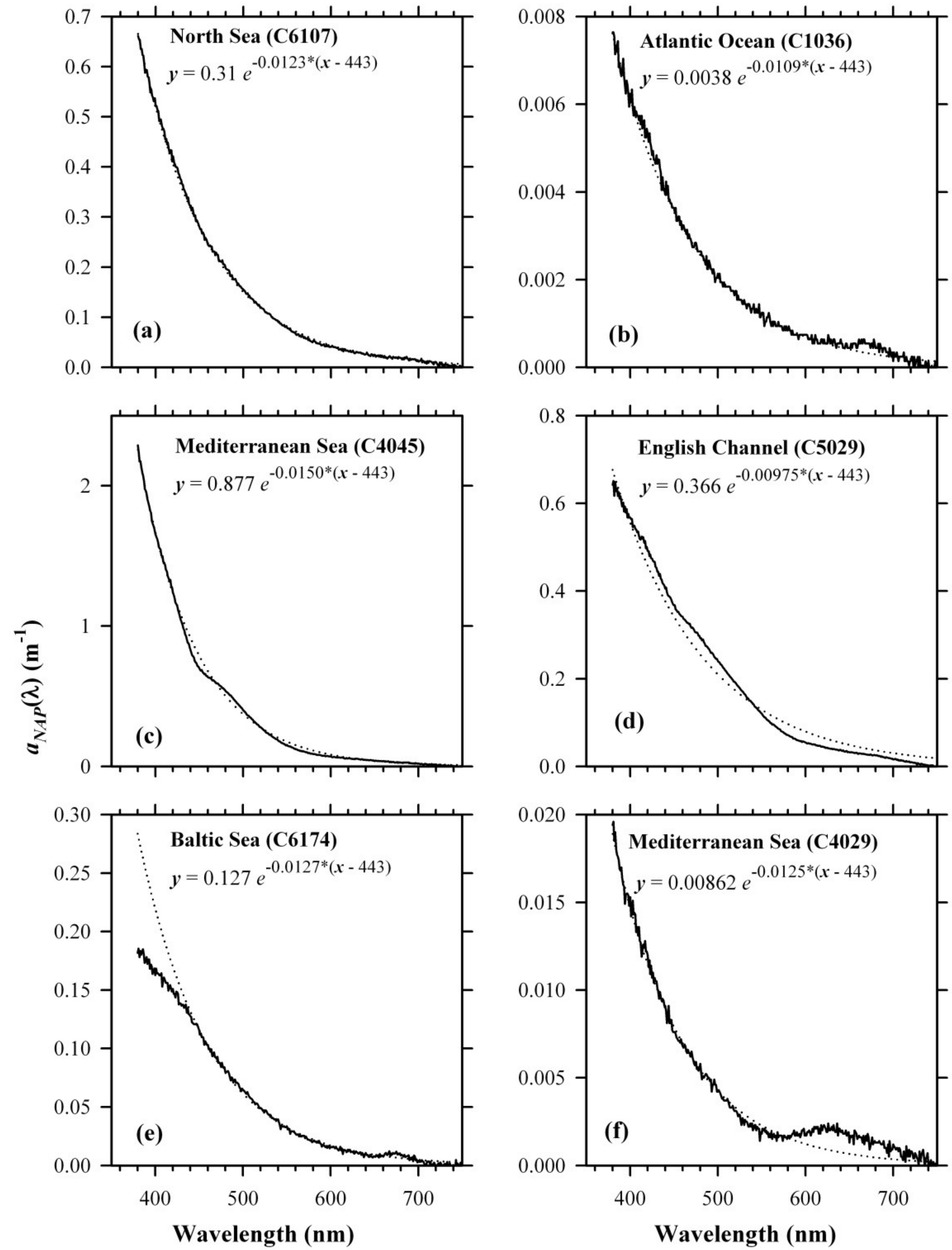

(Babin et al. 2003)

Chlorophyll-based approach

$IOP(\lambda) = IOP_w(\lambda) + f\,[\,Chla\,]$

for example $a_{ph}(\lambda) = f\,[\,Chla\,]$

$a_p(\lambda) = f\,[\,Chla\,]$

$AOP(\lambda)$ (*e.g.*, ocean reflectance) $= f\,[\,Chla\,]$

André Morel
(1933-2012)

Case 1 and Case 2 Waters

CASE 1 WATERS

LIVING ALGAL CELLS
variable concentration

ASSOCIATED DEBRIS
Originating from grazing by zooplankton and natural decay

DISSOLVED ORGANIC MATTER
liberated by algae and their debris (yellow substance)

RESUSPENDED SEDIMENTS
from bottom along the coastline and in shallow areas

TERRIGENOUS PARTICLES
river and glacial runoff

DISSOLVED ORGANIC MATTER
land drainage (terrigenous yellow substance)

ANTHROPOGENIC INFLUX
particulate and dissolved materials

CASE 2 WATERS

Morel and Prieur (1977); Gordon and Morel (1983)

Absorption vs. chlorophyll-a

~ 4-fold variation

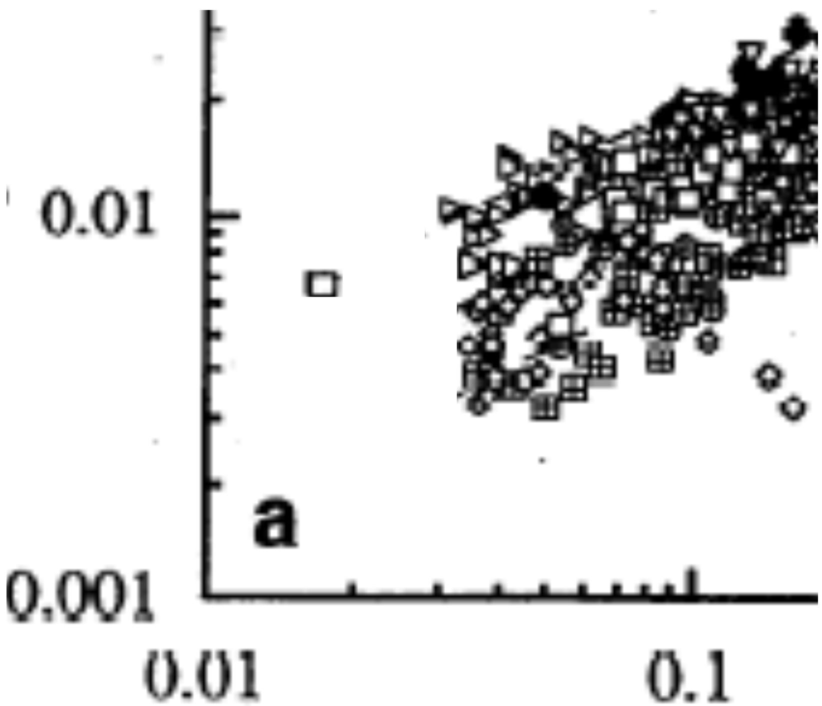

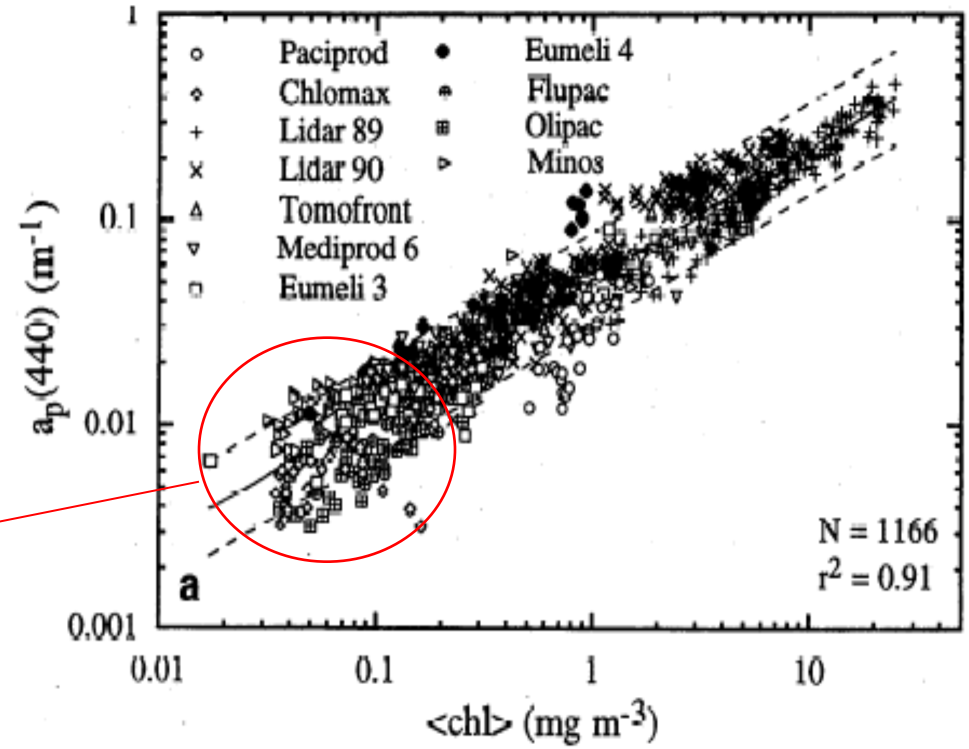

Cruise	Location
PACIPROD	Peru upwelling
CHLOMAX	Sargasso Sea
LIDAR 89	St. Lawrence estuary and gulf
LIDAR 90	St. Lawrence estuary and gulf
TOMOFRONT	northwestern Mediterranean
MEDIPROD 6	southwestern Mediterranean
EUMELI 3	tropical North Atlantic
EUMELI 4	tropical North Atlantic
FLUPAC	equatorial and subequatorial Pacific
OLIPAC	equatorial and subequatorial Pacific
MINOS	eastern and western Mediterranean

(Bricaud et al. 1998)

Beam attenuation vs. chlorophyll-a

> 10-fold variation

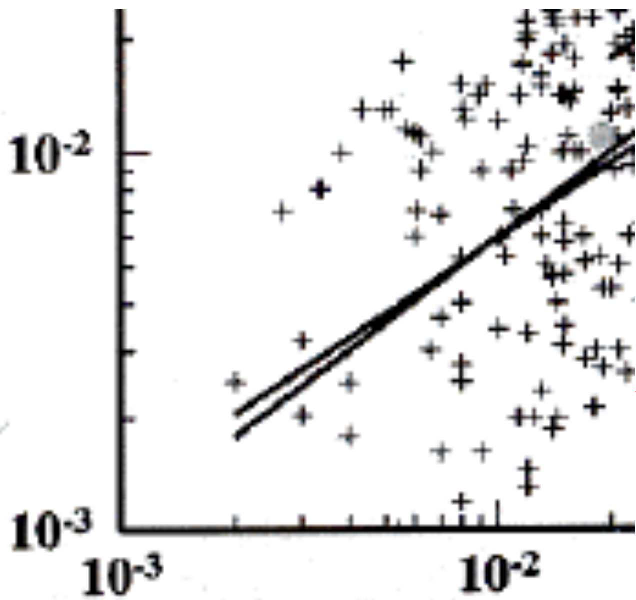

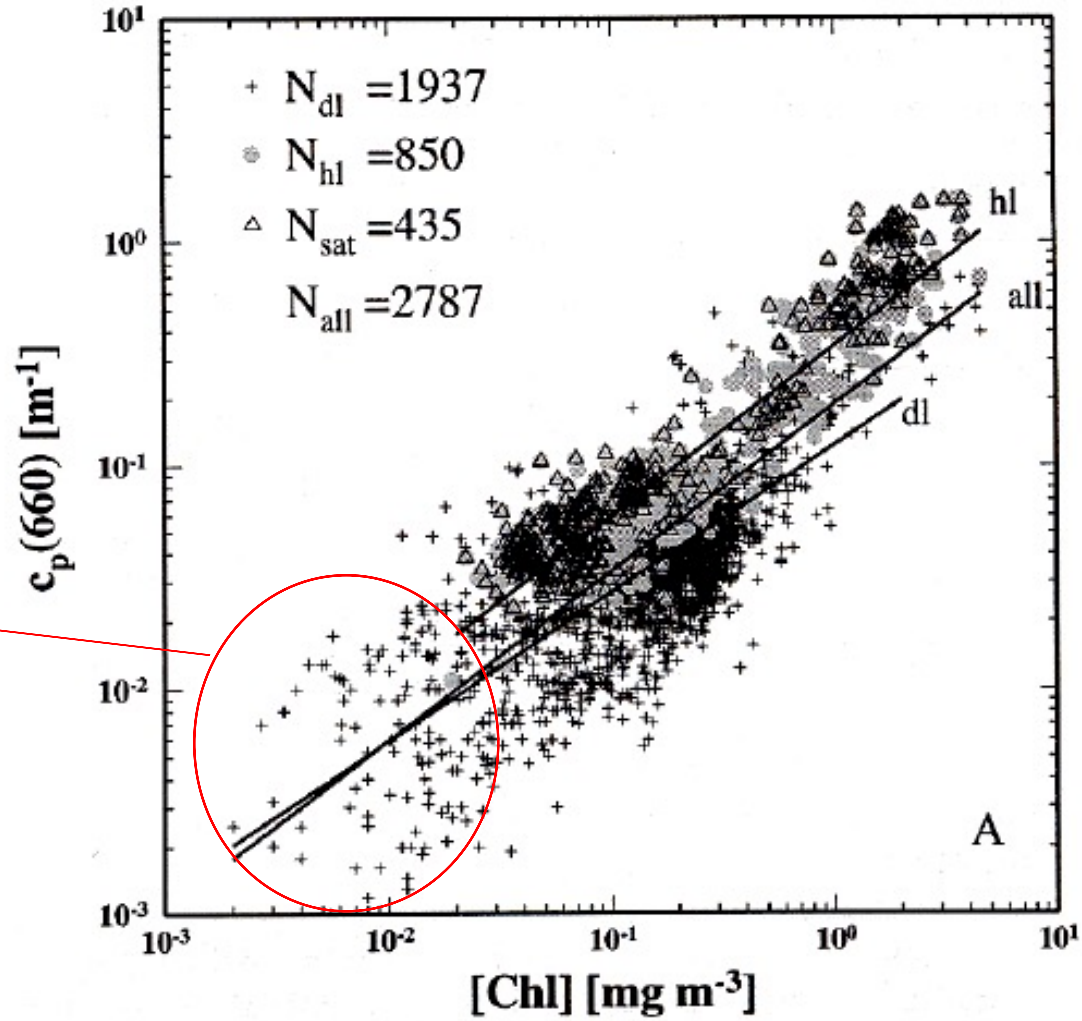

(Loisel and Morel 1998)

Chlorophyll-a algorithm

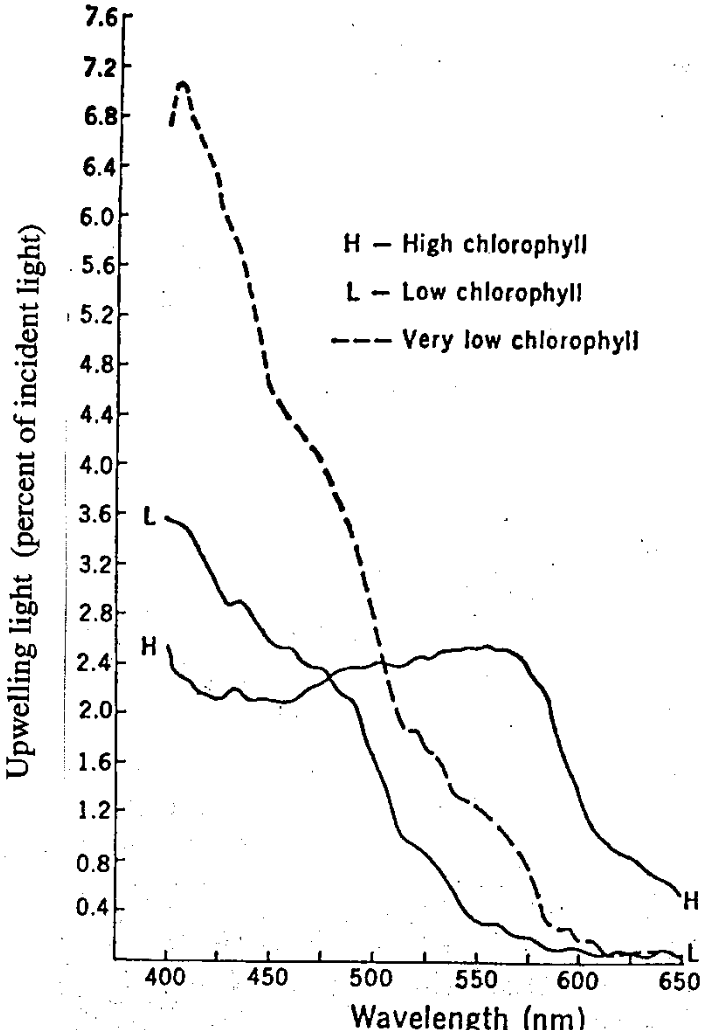

(Clarke, Ewing & Lorenzen 1970)

OC4 Chlorophyll-a algorithm

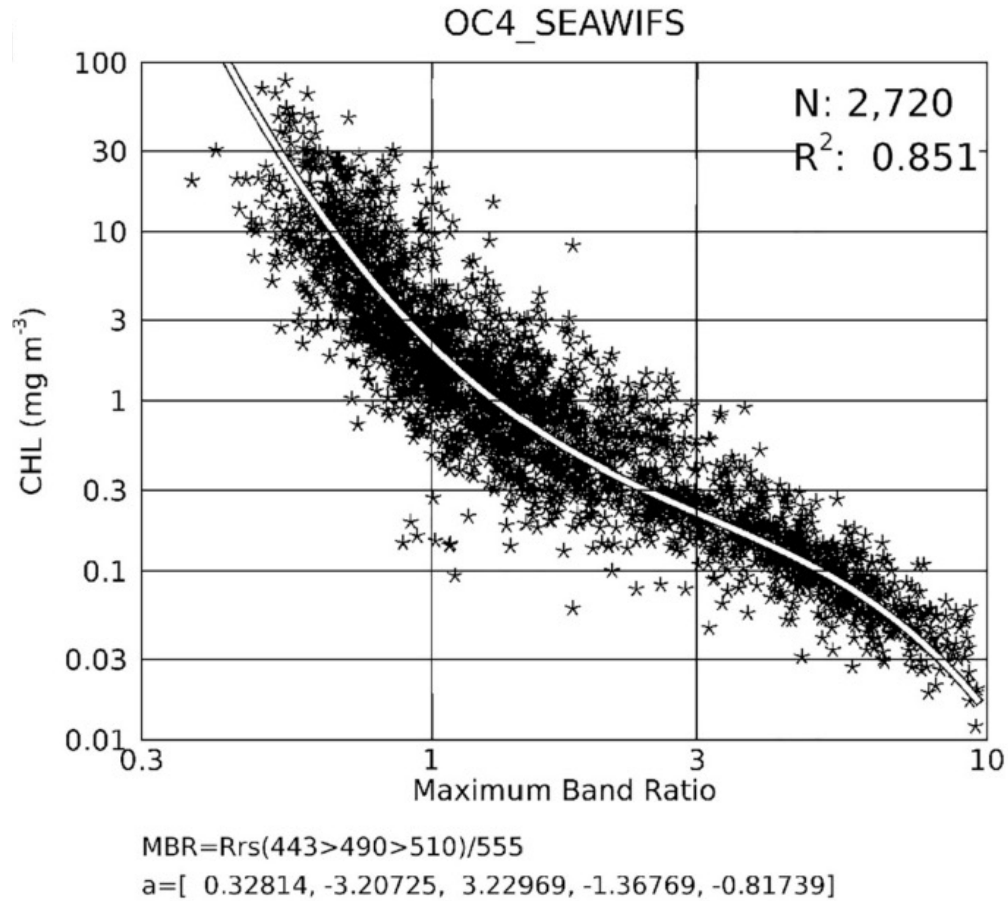

(O'Reilly & Werdell 2019)

Chlorophyll-based approach: Summary

- Parameterization in terms of chlorophyll-a concentration alone
- Empirical regressions (statistically-derived models)
- Provide average trends but no information about variability
- Not valid in Case 2 waters
- Not necessarily satisfactory in Case 1 waters

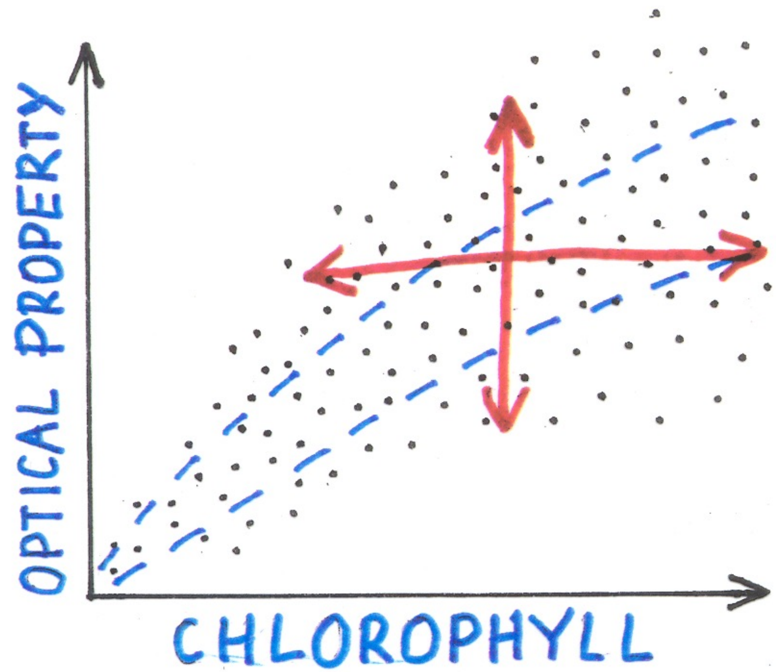

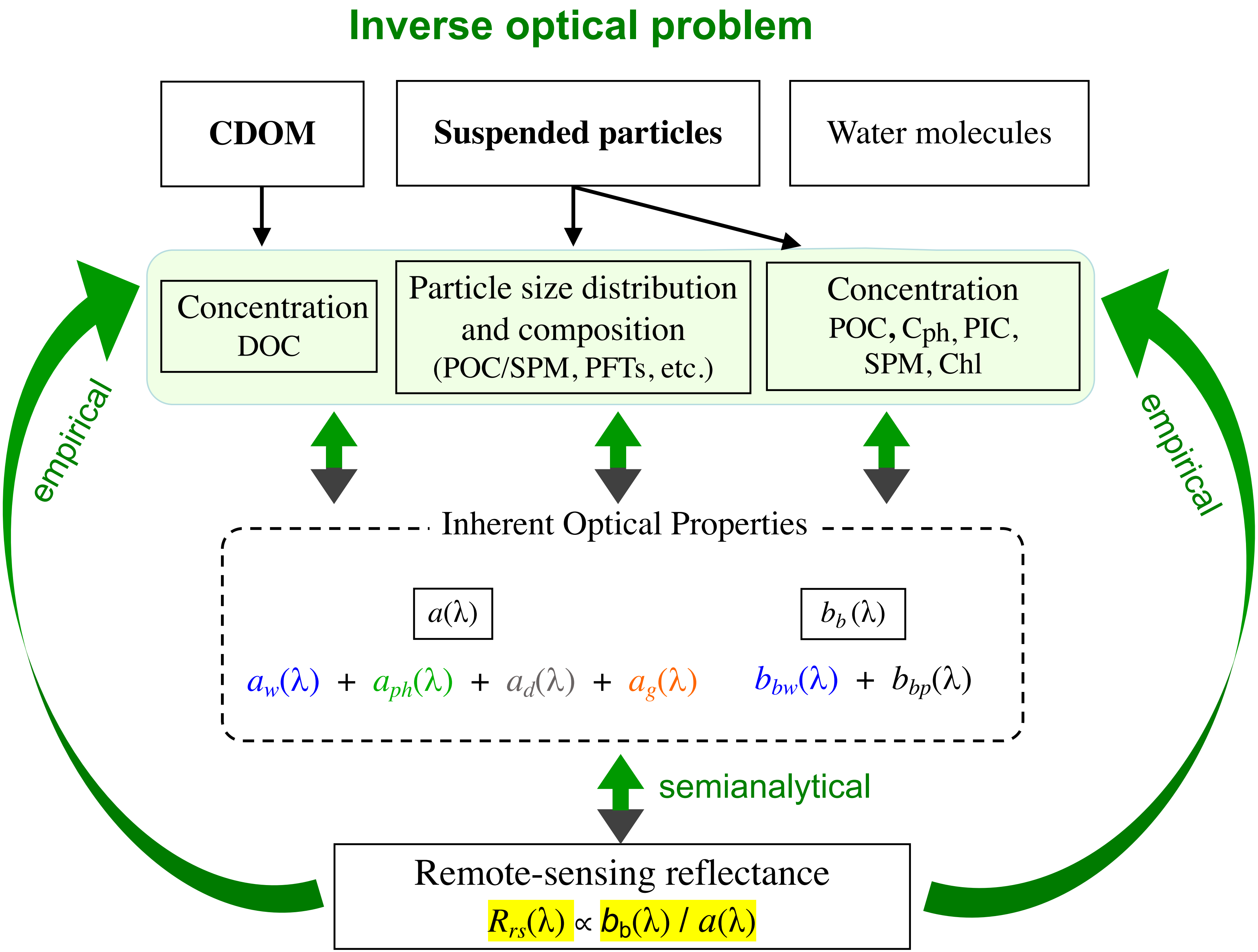

Inverse optical problem
CDOM
Suspended particles
Water molecules
Concentration
DOC
Particle size distribution
and composition
(POC/SPM, PFTs, etc.)
Concentration
POC, C_{ph}, PIC,
SPM, Chl
empirical
empirical
Inherent Optical Properties
$a(\lambda)$
$b_b(\lambda)$
$a_w(\lambda) + a_{ph}(\lambda) + a_d(\lambda) + a_g(\lambda)$
$b_{bw}(\lambda) + b_{bp}(\lambda)$
semianalytical
Remote-sensing reflectance
$R_{rs}(\lambda) \propto b_b(\lambda) / a(\lambda)$

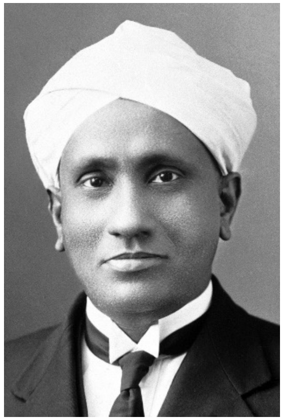

Chandrasekhara Venkata Raman (1988 -1970) Nobel Prize 1930

"In the opinion of the writer, it would make for progress... to recognize that the observed colour of the sea is primarily due to the water itself, and that suspended matter, if present at all in appreciable quantity is to be regarded as a disturbing factor, of which the effect requires to be assessed in each individual case“

Raman, C.V. 1922, "On the molecular scattering of light in water and the colour of the sea", Proc. R. Soc. London A, 101: 64-80

$$Ocean\ Color\ \ R_{rs}(\lambda) \propto \frac{b_b(\lambda)}{a(\lambda)} = \frac{b_{bw}(\lambda)+b_{bp}(\lambda)}{a_w(\lambda)+a_{ph}(\lambda)+a_d(\lambda)+a_g(\lambda)}$$

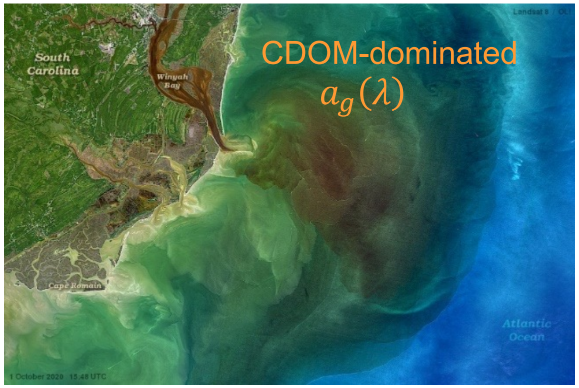

South Carolina coast, Landsat 8 , October 1, 2020 (NASA Ocean Color Web)

Halifax Bay, Eastern Australia
https://blogs.ntu.edu.sg/science/2020/06/24/lights-out-for-muddy-water-coral-reefs-as-global-sea-level-rises/

Phytoplankton-dominated

Coccolithophore bloom, Santa Barbara Channel (https://www.independent.com /2015/ 06/15/ chalk-producing-plankton-turn-ocean-turquoise/)

Microcystis bloom, Lake Erie, July 15, 2019 (https://ocj.com/2021/08/microcystis-cyanobacteria-bloom-monitoring-in-western-lakeerie/

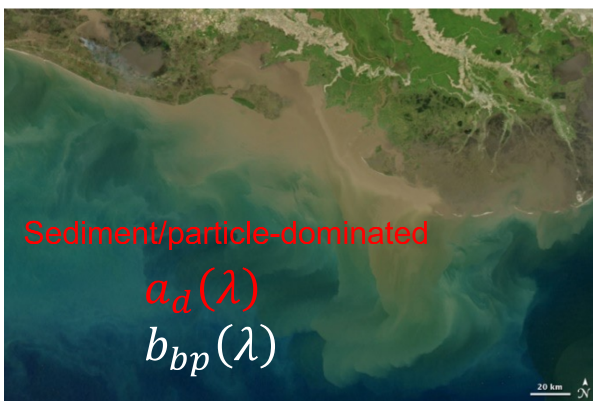

Atchafalaya River plume, Gulf of Mexico, MODIS-Aqua, April 7, 2009 (https://earthobservatory.nasa.gov/ images/ 38273/ sediment-in-the-gulf-of-Mexico)

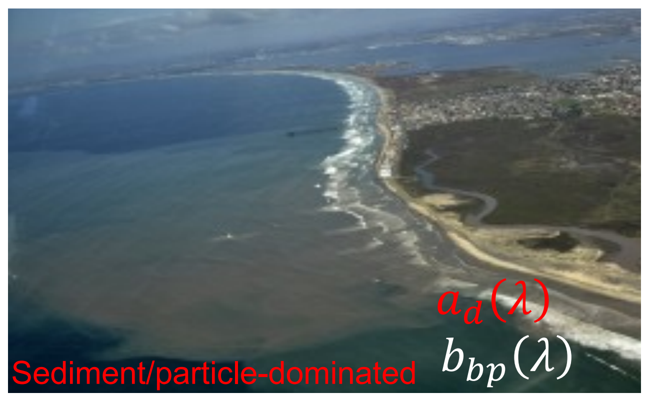

Tijuana River plume, Imperial Beach, California (https://giddingslab.ucsd.edu/research/coastal-ocean/small-plume-dispersion/)

Lingulodinium bloom, off California coast (http://oceandatacenter.ucsc.edu /PhytoGallery/harmful-algae.html)

Reductionist approach

To develop an understanding and assemble a model of the whole, from the reductionist study of its parts

$$IOP_{\mathrm{p}}(\lambda) = \sum_{k} IOP_{k,\,pla}(\lambda) \quad \text{plankton}$$

$$+ \sum_{m} IOP_{m,\,min}(\lambda) \quad \text{minerals}$$

$$+ \sum_{n} IOP_{n,\,det}(\lambda) \quad \text{detritus}$$

The first-order determinant of the bulk IOPs of all plankton microorganisms is the concentration of cells from various species/groups of microorganisms, for example

$a_{all} = \Sigma\, (N/V)_i\, (\sigma_a)_i$ where the sum includes *all* species/groups of microorganisms, each denoted by subscript *i*

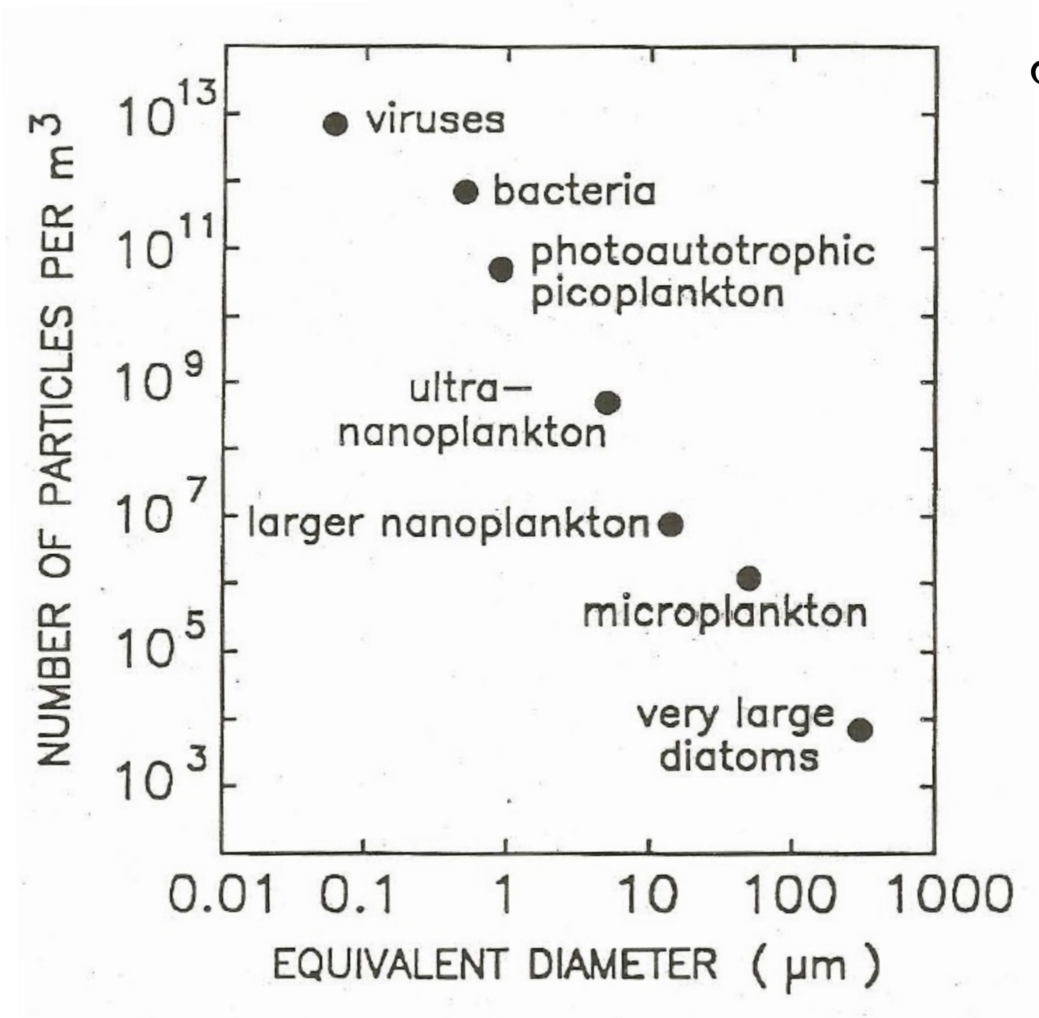

σ_a is the absorption cross section of particle (or biological cell) which is a single-particle optical property dependent on particle physical and chemical characteristics

Example IOP model with detailed description of plankton community

i	Component	Concentration [particles/m^3]	*Chl* [mg m^{-3}]
1	VIRU	$1.0 \cdot 10^{13}$	0
2	HBAC	$4.0 \cdot 10^{11}$	0
3	PROC	$7.0 \cdot 10^{10}$	0.1026
4	SYNE	$2.0 \cdot 10^{10}$	0.0403
5	SYMA	$8.0 \cdot 10^{9}$	0.0360
Σ	Picoplankton	$4.98 \cdot 10^{11}$	0.1789
6	PING	$4.5056 \cdot 10^{8}$	0.0540
7	PSEU	$0.9808 \cdot 10^{8}$	0.0303
8	LUTH	$0.9924 \cdot 10^{8}$	0.0107
9	GALB	$0.4839 \cdot 10^{8}$	0.0155
10	HUXL	$0.4339 \cdot 10^{8}$	0.0104
11	CRUE	$0.4496 \cdot 10^{8}$	0.0129
12	FRAG	$0.4768 \cdot 10^{8}$	0.0157
13	PARV	$0.6247 \cdot 10^{8}$	0.0181
14	BIOC	$0.3966 \cdot 10^{8}$	0.0900
15	TERT	$0.3570 \cdot 10^{8}$	0.0609
16	CURV	$0.2987 \cdot 10^{8}$	0.0099
Σ	Small Nanoplankton	$1.0 \cdot 10^{9}$	0.3284
17	ELON	$1.7 \cdot 10^{7}$	0.1595
18	MICA	$2.0 \cdot 10^{6}$	0.0508
Σ	Total Plankton	$1.0499019 \cdot 10^{13}$	0.7176
19	DET	$3.3 \cdot 10^{14}$	0
20	MIN	$1.1 \cdot 10^{14}$	0
Σ	Total Non-living Particles	$4.4 \cdot 10^{14}$	0
21	BUB	$7.1 \cdot 10^{6}$	0

(Stramski et al. 2001)

Size distribution

18 planktonic components
composite plankton
mineral particles
organic detritus
air bubbles

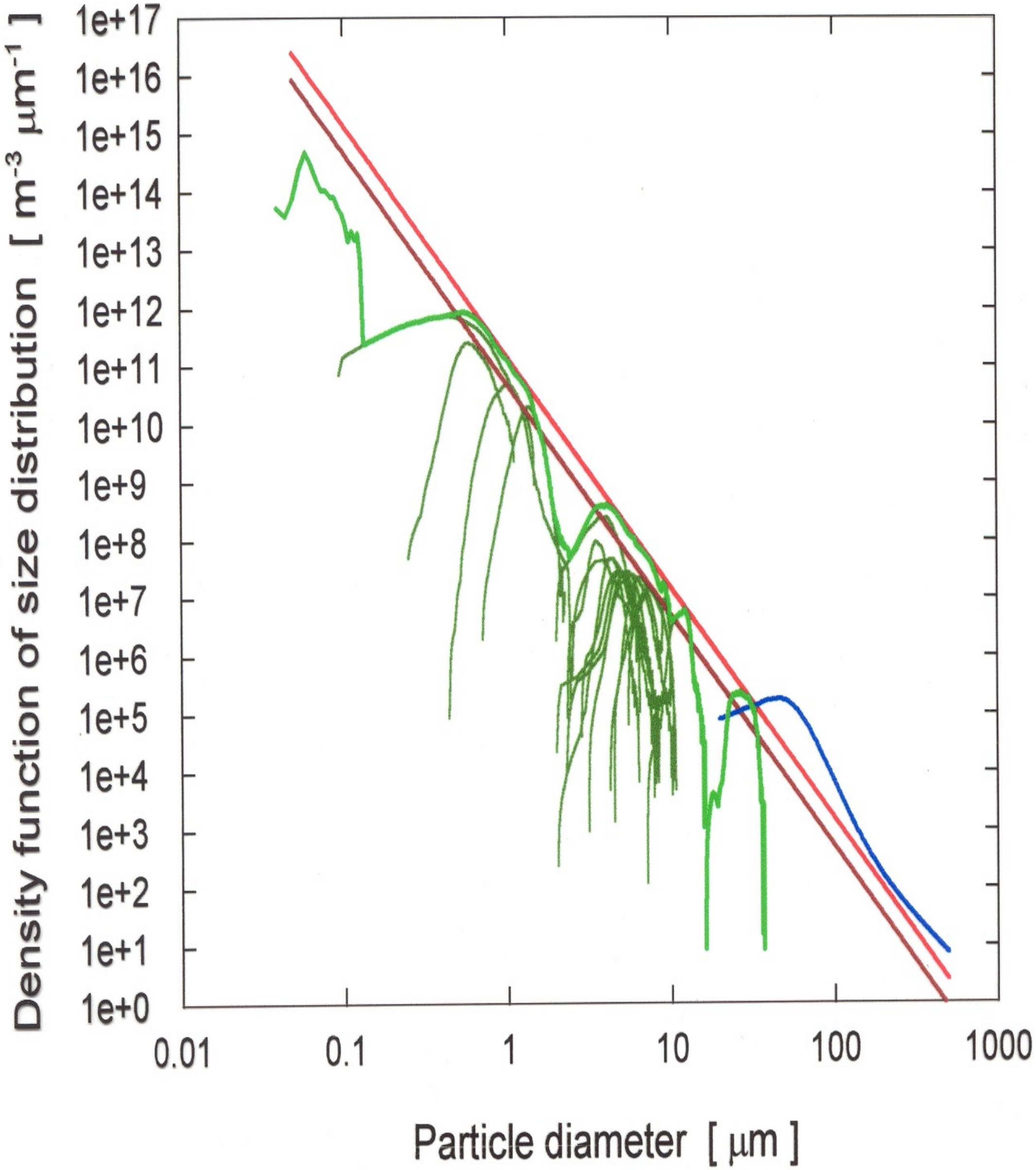

(Stramski et al. 2001)

Absorption budget

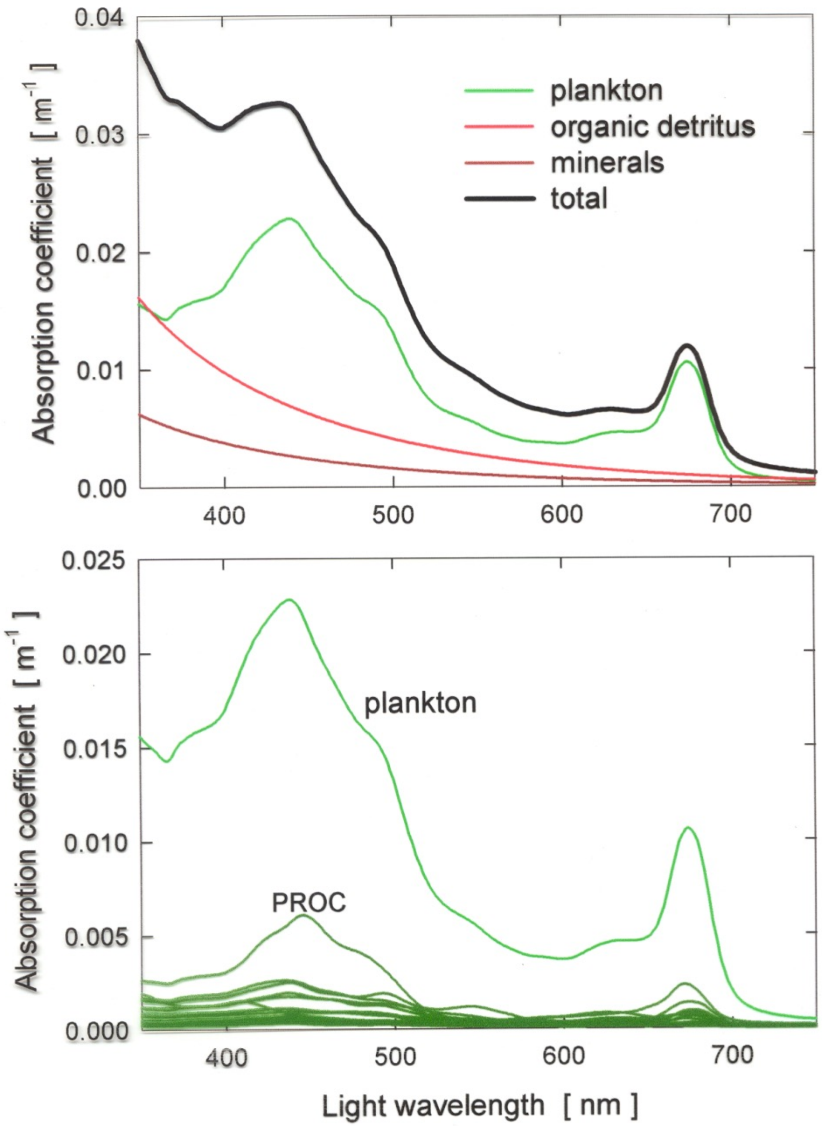

Scattering budget

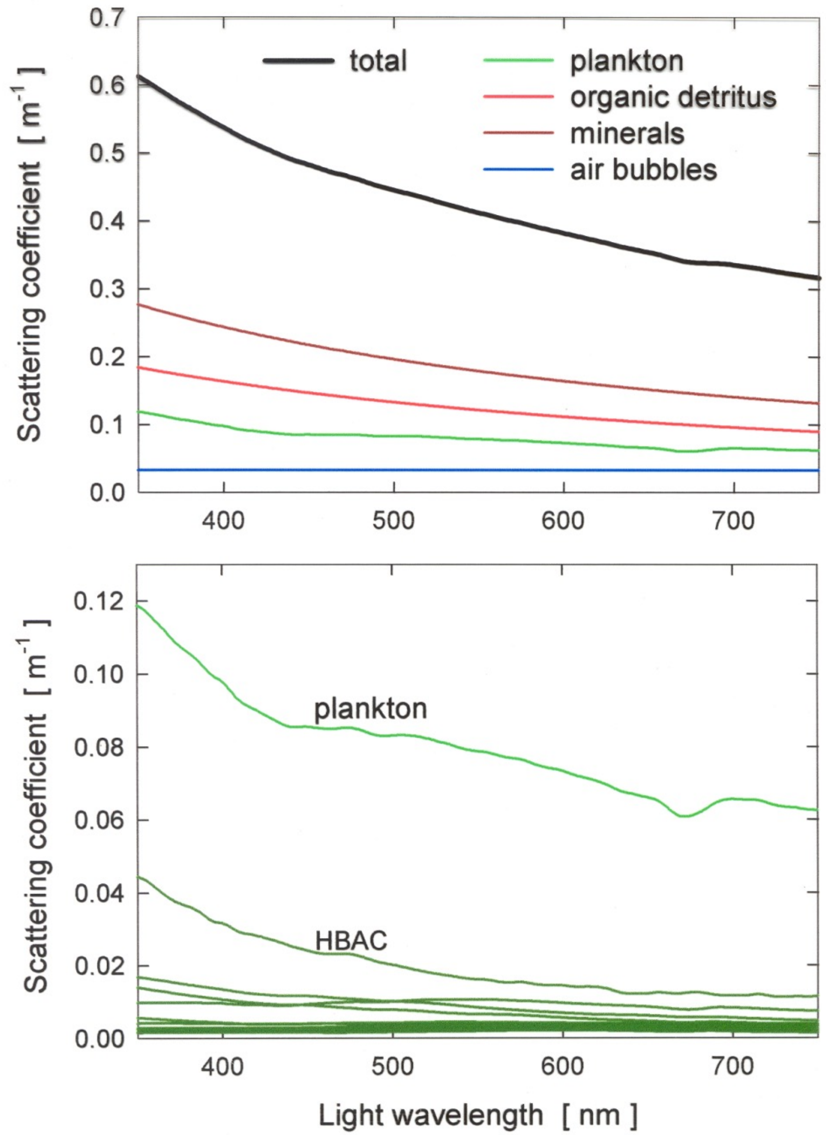

(Stramski et al. 2001)

Reductionist radiative transfer/reflectance model

Input to radiative transfer model

$$IOP(\lambda) = \sum_{i=1}^{j} IOP_i(\lambda) = \sum_{i=1}^{j} N_i \overline{\sigma_i}(\lambda)$$

Output, *e.g.* ocean reflectance

$$R(\lambda) = f\,[\sum_{i=1}^{j} N_{\mathrm{i}} \overline{\sigma}_{i,a}(\lambda), \sum_{i=1}^{j} N_{\mathrm{i}} \overline{\sigma}_{i,b}(\psi, \lambda)]$$

- In what ways does variability in detailed seawater composition determine variability in ocean reflectance?
- What information about water constituents and optical properties can we hope to extract from remotely sensed reflectance?

Example combination of reductionist IOP model and radiative transfer model for simulating ocean color

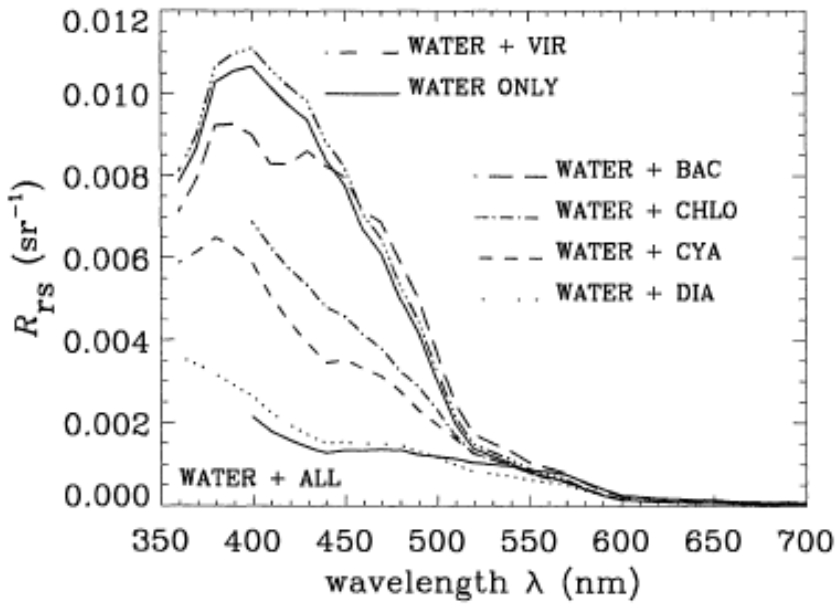

Viruses (~0.07 μm in size)
Heterotrophic bacteria (~0.5 μm)
Cyanobacteria (~1 μm)
Small diatoms (~4 μm)
Chlorophytes (~8 μm)
Detritus
CDOM

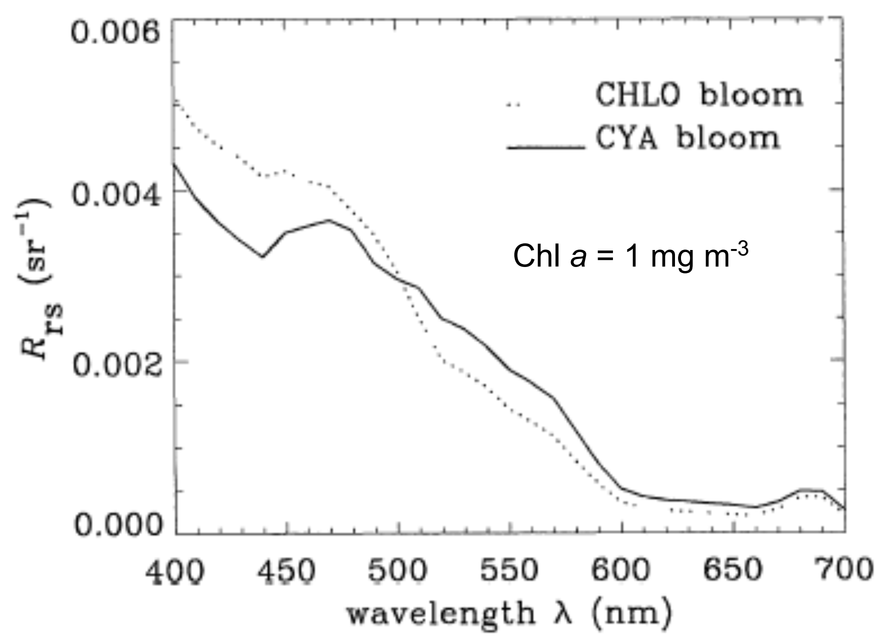

Stramski and Mobley (1997)
Mobley and Stramski (1997)

The complexity of seawater as an optical medium should not deter us from pursuing the proper course in future research

“The reductionist worldview has to be accepted as it is, not because we like it, but because that is the way the world works”

Steven Weinberg

1979 Nobel Prize in Physics